

Holographic correlation functions from wedge

Tengzhou Lai^{a,1}, Ya-Wen Sun^{a,c,2}, Jia Tian^{b,c,3}

^a*School of Physical Sciences, University of Chinese Academy of Sciences,
Zhongguancun East Road 80, Beijing 100190, P. R. China*

^b*State Key Laboratory of Quantum Optics and Quantum Optics Devices, Institute of
Theoretical Physics, Shanxi University, Taiyuan 030006, P. R. China*

^c*Kavli Institute for Theoretical Sciences (KITS), University of Chinese Academy
of Science, 100190 Beijing, P. R. China*

Abstract

In this work, we propose a novel holographic method for computing correlation functions of operators in conformal field theories. This method refines previous approaches and is specifically aimed at being applied to heavy operators. For operators that correspond to particles in the bulk, we show that the correlation functions can be derived from the on-shell actions of excised geometries for heavy operators, using numerical and perturbative calculations. These excised geometries are constructed from various background solutions such as Poincaré AdS₃, global AdS₃, and BTZ by cutting out a wedge bounded by two intersecting End-of-the-world branes and the AdS boundary. The wedge itself can be interpreted as a dual to a BCFT with cusps in the AdS/BCFT framework. Additionally, we calculate the correlation functions for heavy operators directly by constructing backreacted bulk geometries for particle excitations through coordinate transformations from a conical solution. We find that the on-shell actions of these backreacted solutions accurately reproduce correlation functions, although they differ from those computed in Fefferman-Graham(FG) gauge. This discrepancy, previously noted and explained in our earlier work, is reinforced by additional examples presented here.

¹laitengzhou20@mailsucas.ac.cn

²yawen.sun@ucas.ac.cn

³wukongjiaozi@ucas.ac.cn

Contents

1	Introduction	1
2	The Wedge proposal of correlation functions	3
2.1	A toy model	4
2.2	AdS/BCFT with corners	6
3	Cases study	9
3.1	Poincaré AdS ₃	10
3.2	Global AdS ₃	12
3.3	BTZ	15
4	Backreacted geometries	21
4.1	The on-shell action	23
5	Discussion	31
A	Wedge in Poincaré AdS₃	33
B	The detail of the integral	34
C	Higher-order corrections	36

1 Introduction

Over the past few decades, string theory has been the most popular candidate for a quantum theory of gravity. One of its most significant implications is the AdS/CFT correspondence [1–3], which states that a quantum gravity theory living in the bulk AdS_{d+1} space is dual to a conformal field theory CFT_d defined on the asymptotic AdS boundary. Various aspects of this correspondence have been validated [4–8], with a crucial task being the understanding of the holographic dual of correlation functions, which are fundamental observables in conformal field theories. The standard method for computing correlation functions is encapsulated in the GKPW dictionary [3, 9]:

$$Z_{\text{AdS}}(\phi_{\partial} = \phi_0) = \left\langle \exp \left(\int \phi_0 \mathcal{O} \right) \right\rangle_{\text{CFT}} \quad (1.1)$$

where the boundary value of a bulk field provides the source for the dual operator inserted on the boundary CFT. However, an implicit assumption in this framework is that the ADM mass of the bulk field, or the scaling dimension of the dual primary operator, remains of constant order, specifically $\Delta \sim \mathcal{O}(1) \ll \frac{\ell^{d-1}}{G_N}$. This condition implies that the backreaction from the bulk fields is negligible, allowing for reliable calculations [10] and conclusions based on a fixed background. When the scaling dimension of the dual operator increases

but remains bounded such that $\mathcal{O}(1) \ll \Delta \ll \frac{\ell^{d-1}}{G_N}$, the corresponding correlation function can be approximated using a classical saddle point or WKB approximation [11–13]:

$$\langle \mathcal{O}(x_1) \mathcal{O}(x_2) \rangle = \int_{\mathcal{P}} D[\mathcal{P}] e^{-\Delta L(\mathcal{P})} \sim \sum_{\text{geodesics}} e^{-\Delta L(x_1, x_2)} \quad (1.2)$$

where \mathcal{P} represents arbitrary bulk path connecting two insertions and $L(\mathcal{P})$ is the corresponding regularized length functional. Once the scaling dimension of the dual operator approaches the CFT central charge, i.e., $\Delta \sim \frac{\ell^{d-1}}{G_N}$, the backreaction on the bulk geometry becomes significant, and the on-shell action encodes all pertinent information about the correlation functions or a specific conformal block [14–18]. Recently, a spacetime banana proposal was introduced in [19, 20], refined and generalized in [21], for computing correlation functions of so-called huge operators that are sufficiently heavy to deform the geometry into a black hole.

However, usually constructing backreacted geometries is a very challenging task. A relatively simple situation is when the inserted operators are dual to massive particles, where the backreacted geometries are described by conical solutions. Nevertheless, for the purpose of calculating correlation functions, we need to perform a coordinate transformation to transform the geometry to a form in accordance with the calculation of the two-point function, with the trajectory of the particle excitation connecting the two spacetime points where the boundary operators are located. The explicit metric after this transformation is still very hard to find, especially when we calculate higher points correlation functions. One resolution is based on the fact that the solution near the boundary is fixed by its behaviors around each boundary insertion point. As a result, its on-shell action can be directly computed with no need of the details of the whole metric [22, 23] and it turns out the action reduces to the one of a Liouville theory [20, 24].

In this paper, to resolve this problem we propose a more direct approach to compute the on-shell actions of conical solutions by leveraging the fact that these geometries can be constructed through a cut-and-glue procedure [11, 25, 26]. We demonstrate that the correlation functions could be read from the on-shell action of an excised geometry, thereby confirming the cut-and-glue construction at the level of matching on-shell actions. More specifically, our proposal is quantitatively expressed as ⁴

$$I^{BR} = I^{AdS_3} - I_{gravity, W} + I_m \quad (1.3)$$

where the left-hand side represents the on-shell action of a general backreacted conical geometry with bulk particle excitations, and the right-hand side corresponds to the excised geometry. It is important to note that this equivalence has been examined in [27] for a specific example, and a two-point correlation function could be read from the on-shell action in this way. In this work, based on their discoveries, we formulate this wedge proposal explicitly, and utilize this equivalence at the level of the on-shell action to derive

⁴The meaning of each term will be clarified in the next section.

the two-point correlation function of dual heavy operators. The correct form of correlation functions obtained further confirm this equivalence and the correctness of this wedge proposal, with the hope of generalizing it to higher-point correlation function in future studies.

We will explore this wedge proposal across various AdS₃ solutions, highlighting caveats and subtleties. Though the wedge proposal could, in principle, be generalized to higher dimensions, the advantage of focusing on AdS₃ solutions lies in the fact that conical geometries associated with bulk particle excitations can be obtained through coordinate transformations in three dimensions, as demonstrated in [28]. Therefore, we can verify the wedge proposal through this direct calculation, motivating us to also directly compute the two-point functions in the backreacted geometries. In our previous study [21] on the on-shell action for the backreacted Poincaré geometry, an unexpected result was uncovered: the on-shell actions of the backreacted geometry in transformed coordinates differ from those in FG [29, 30] coordinates. Here in all direct calculations of the two-point functions in the backreacted geometries, we will show that this discrepancy is common and manifests in all examined examples.

The outline of this paper is listed as follows: in section 2, we give our wedge proposal of correlation functions and relate it to the AdS/BCFT formalism [31, 32]; then in section 3, we analytically compute the on-shell action inside a wedge region case by case in various AdS₃ spacetime both analytically and numerically, and confirm their consistence. The result obtained successfully reproduces the two-point correlation function. In section 4, we straightforwardly construct backreacted geometries and compute the on-shell action both in the whole coordinate patch and the FG patch. In section 5, we briefly discuss our result and give a few future directions.

2 The Wedge proposal of correlation functions

In this section, we propose a novel holographic approach to compute the correlation functions of operators in conformal field theories (CFTs). Our method integrates two key insights recently revisited in [27] and [19–21]. Firstly, the correlation functions or conformal blocks can be derived from the on-shell action of gravity on specific conical geometries for heavy operators corresponding to particle excitations in the bulk. For instance, as discussed in [19–21], the holographic dual of the two-point function can be constructed from the standard conical AdS solution by applying a global to Poincaré (GtP) transformation [20]

$$r = \frac{R}{z}, \quad \tau = \frac{1}{2} \log(R^2 + z^2) \quad (2.1)$$

followed by a special conformal transformation(SCT). Secondly, it is well established that a conical geometry can be interpreted as a wedge of the global AdS geometry or equivalently as the global AdS geometry with a wedge region excised [11, 25, 26].

Combining these two insights suggests that the correlation functions may also be calculated from the on-shell action of a bulk geometry with a specific wedge excised. This

idea, to our knowledge, was first articulated in [33], albeit with some caveats, which we will review below. In this paper, we aim to explore more general scenarios. A subtlety in the wedge construction of conical geometry is the lack of rigorous proof that the equivalence between the excised geometry and the conical geometry holds at the level of the on-shell action. It turns out that to assert this equality, additional terms must be added to the action of the gravity theory. For instance, to accurately describe a spacetime wedge, it is more appropriate to employ the AdS/BCFT formalism, as the wedge possesses spacetime boundaries. Furthermore, the tip of the wedge represents another type of spacetime singularity, which also necessitates consideration in the action.

The advantage of our wedge approach is that it circumvents the need to construct the specific backreacted geometry for the calculation of the correlation functions with operator insertions, which is often a challenging task. For example, we can conveniently utilize the wedge construction to describe the formation of a black hole through the collision of two particles [25].

2.1 A toy model

To illustrate these issues, let us consider a toy model: the conical AdS which has the metric

$$ds^2 = (r^2 + \alpha^2) d\tau^2 + \frac{dr^2}{r^2 + \alpha^2} + r^2 d\theta^2, \quad \theta \sim \theta + 2\pi. \quad (2.2)$$

The geometry is not smooth but has a conical singularity at $r = 0$ with a deficit angle $2\pi(1 - \alpha)$, which can be thought of as the backreaction of a massive particle that is dual to a heavy operator in the boundary field theory, so the total action of the system is

$$I_{\text{grav}} = -\frac{1}{16\pi G_N} \int_{\mathcal{M}} \sqrt{g} (R + 2) - \frac{1}{8\pi G_N} \int_{\partial\mathcal{M}} \sqrt{h} (K - 1) + m \int_{\Gamma} \sqrt{\gamma}, \quad (2.3)$$

where Γ represents the trajectory of the particle and m is the local mass of the particle. In particular, the profile Γ is stationary and along with the AdS center in this case, the mass and the deficit angle is related by the component of Einstein equation [34] along the trajectory

$$R_{\tau\tau} - \frac{1}{2} g_{\tau\tau} R - g_{\tau\tau} = -2\pi (1 - \alpha) \delta_{\Gamma} g_{\tau\tau} \quad (2.4)$$

which implies that

$$m = \frac{1 - \alpha}{4G_N}. \quad (2.5)$$

Therefore, the on-shell action equals

$$I_{\text{grav}} = -\frac{1}{16\pi G_N} \int_{\mathcal{M}/\Gamma} \sqrt{g} (R + 2) - \frac{1}{8\pi G_N} \int_{\partial\mathcal{M}} \sqrt{h} (K - 1), \quad (2.6)$$

$$= \frac{1}{4\pi G_N} \int_{\partial\mathcal{M}} \left(\frac{\Lambda^2 - \epsilon^2}{2} \right) - \frac{1}{8\pi G_N} \int_{\partial\mathcal{M}} \left(\Lambda^2 + \frac{\alpha^2}{2} \right) \quad (2.7)$$

$$= -\frac{\alpha^2}{16\pi G_N} WT = -\frac{\alpha^2}{8G_N} \xi, \quad (2.8)$$

where $W = 2\pi$ is the width of the boundary cylinder, T is the length of the boundary cylinder and $\xi = 2\pi T/W$ is the dimensionless modular parameter. From the on-shell action, we read off the excitation energy due to the particle insertion is $E = (-\frac{\alpha^2}{8G_N}) - E_0 = -\frac{c}{12}\alpha^2 + \frac{c}{12} = \frac{c}{12}(1 - \alpha^2)$, where the relation $\frac{1}{2G_N} = \frac{c}{3}$ [35] and the vacuum energy is $-\frac{c}{12}$ have been used.

Another description of the backreaction on the geometry is to excise a bulk wedge with angle $2\pi(1 - \alpha)$ [11, 25] from the global AdS geometry. To describe the wedge, we consider the

$$I_{\text{gravity},W} = -\frac{1}{16\pi G_N} \int_{\mathcal{M}} \sqrt{g}(R + 2) - \frac{1}{8\pi G_N} \int_{\partial\mathcal{M}} \sqrt{h}(K - 1) - \frac{1}{8\pi G_N} \int_{Q_1 \cup Q_2} \sqrt{h}(K - T) - \frac{1}{8\pi G_N} \int_{\Gamma} \sqrt{\gamma} \cos^{-1}(n_1 \cdot n_2) - \frac{1}{8\pi G_N} \int_{Q_{1,2} \cap \partial\mathcal{M}} \sqrt{\gamma} \cos^{-1}(n_{1,2} \cdot n_0) \quad (2.9)$$

where $n_{1,2}$ denotes the normal vectors to the End of the world(EOW) branes $Q_{1,2}$ ($\theta = \pm\pi(1 - \alpha)$) with tension $T = 0$, while n_0 represents the normal vector to the asymptotic boundary. As a result, the boundaries $Q_{1,2}$ of wedge do not contribute to the action. Additionally, since the EOW branes are perpendicular to the AdS boundary, the Hayward terms [36] at $Q_{1,2} \cap \partial\mathcal{M}$ do not contribute either. The only non-trivial term is the corner term at the tip of the wedge⁵

$$I_{\text{Hayward}} = -\frac{1}{8\pi G_N} \int_{\Gamma} \sqrt{\gamma} \cos^{-1}(n_1 \cdot n_2) = -\frac{1}{8\pi G_N} \int_{\Gamma} \sqrt{\gamma} (\pi - 2\pi(1 - \alpha) - \pi) = \frac{1 - \alpha}{4G_N} \int_{\Gamma} \sqrt{\gamma}, \quad (2.10)$$

which precisely cancels the mass term associated with the particles. Therefore, the on-shell action is

$$I^{AdS_3} - I_{\text{gravity},W} + I_m = -\frac{1}{16\pi G_N} WT = -\frac{\alpha^2}{8G_N} \xi, \quad (2.11)$$

where the modular parameter $\xi = 2\pi T/W$ and $W = 2\pi\alpha$. Thus, comparing (2.8) with (2.11) reveals that these two descriptions agree with each other on the level of on-shell action. The important lesson is that in both descriptions, the mass term always gets canceled by the term that describes the conical singularity [38]. It means when we compute the on-shell action, we do not consider them⁶. Before delving into the wedge constructions, let us first introduce the theory for properly describing the wedge.

⁵Here, due to the identification of these two edges, we should subtract an overall angle of π as in [33, 37].

⁶For convenience, we will use $I_{\text{gravity},W}$ to represent $I_{\text{gravity},W} - I_m$ in the following context.

2.2 AdS/BCFT with corners

The proper theory for describing a wedge is the generalized AdS/BCFT duality in which the EOW branes are connected or intersected along a defect. The action of the gravity model is given by

$$I = -\frac{1}{16\pi G_N} \int_{\mathcal{M}} \sqrt{g}(R+2) - \frac{1}{8\pi G_N} \int_{\text{EOW}} \sqrt{h}(K-T) + \frac{1}{8\pi G_N} \int_{\Gamma} (\theta - \theta_0) \sqrt{\gamma}, \quad (2.12)$$

where the last term is the analog of the Hayward term and θ_0 is a fixed value that characterizes the corner. This generalization was introduced in [39–42], and further explored in [43] (also see our companion paper [21] for a novel application). With this generalization, we can construct a holographic dual of a boundary-condition-changing (BCC) operator [44, 45], defined as the primary state with the lowest conformal dimension in a BCFT defined on an interval with a pair of different boundary conditions. In the standard AdS/BCFT framework, the gravitational description of a BCFT on an interval $\theta \in [0, \pi]$ in the low-temperature phase is the global AdS₃ solution with the metric

$$ds^2 = (r^2 + 1)d\tau^2 + \frac{dr^2}{r^2 + 1} + r^2 d\theta^2, \quad \theta \sim \theta + 2\pi. \quad (2.13)$$

The two boundaries at $\theta = 0, \pi$ correspond to a EOW brane with the profile function

$$r \sin \theta = -\lambda, \quad \lambda \equiv \frac{T}{\sqrt{1 - T^2}} \quad (2.14)$$

where T is the tension of the brane. Obviously, the EOW brane intersects the AdS boundary at the $\theta = 0$ and $\theta = \pi$ as desired. Because the two boundaries are connected by the same EOW brane, effectively, we are imposing the same conformal boundary condition on them. Therefore, the BCC operator in this case is just the identity operator. To verify this, we can compute the on-shell action (2.12) of this bulk solution, the result is

$$I = -\frac{\beta}{16G_N} = -\frac{c}{24}\beta, \quad (2.15)$$

where β is the size of the τ -circle. Recall that the vacuum energy of is $E_0 = -\frac{c}{24}$, we conclude that the conformal dimension of the BCC operator is $-\frac{c}{24} - E_0 = 0$, indicating that the BCC operator here is the identity operator.

To find the gravity dual of a non-trivial BCC operator, as shown in [41, 42], we should consider the conical AdS₃ bulk solution with the metric (2.2). The EOW brane in the conical AdS geometry has the general profile

$$r \sin[\alpha(\theta - \theta_0)] = -\alpha\lambda, \quad \theta \in (\theta_0, \theta_0 + \frac{\pi}{\alpha}). \quad (2.16)$$

Therefore, requiring that the two boundaries of the BCFT are still at $\theta = 0, \pi$, we have to use two EOW branes. This is illustrated in Figure 1. Without the loss of generality, we can choose the two EOW branes to be

$$r \sin(\alpha\theta) = -\alpha\lambda_1, \quad r \sin(\alpha(\theta - \pi)) = -\alpha\lambda_2, \quad (2.17)$$

which intersect in the bulk at two positions $\theta = \theta_*, \theta_* + \pi$ and we will choose the shaded region in Figure 1 as the bulk dual. The intersection angle is not important to us, the

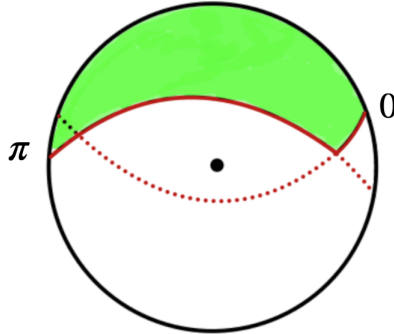


Figure 1: The bulk dual of a non-trivial BCC operator.

point is that there always exists $T_{i=1,2}$ for such an intersection to happen. The on-shell action of this solution is given by

$$I = -\frac{c\alpha^2}{24}\beta, \quad (2.18)$$

which implies that the conformal dimension of the BCC operator is

$$h_{bcc} = \frac{c}{24}(1 - \alpha^2), \quad \Delta_{bcc} = 2h_{bcc} = \frac{c}{12}(1 - \alpha^2). \quad (2.19)$$

Note that for our choice of the bulk dual, the conical singularity at the center of AdS space is not included, so the BCC operator is solely dual to the defect which stays in the bulk. Assuming $\beta \rightarrow \infty$, then one can think that the BCC operators ϕ_i are inserted at $\tau = -\infty$ and $\tau = \infty$ such that the partition function is given by

$$Z = e^{-I} = \langle \phi | e^{-\beta(L_0 - \frac{c}{24})} | \phi \rangle = e^{-\beta(h_{bcc} - \frac{c}{24})}. \quad (2.20)$$

In this paper, we are interested in another type of gravity solutions where the defect can intersect with the AdS boundary. We expect that such solutions correspond to the correlation functions of BCC operators. First, let us recall some known facts about the correlation function of BCC operators. Two-point function of BCC operators on a disk of radius β (see figure 2) is given by [46]⁷

$$\langle \mathcal{O}_{J_1 J_2}(0) \mathcal{O}_{J_2 J_1}(\tau) \rangle_{\text{disk}} = \left(\frac{\pi \epsilon}{\beta \sin(\pi \tau / \beta)} \right)^{2\Delta[J_2, J_1]} \quad (2.21)$$

which in the limit $\tau/\beta \rightarrow 0$ is approximately

$$\langle \mathcal{O}_{J_1 J_2}(0) \mathcal{O}_{J_2 J_1}(\tau) \rangle_{\text{disk}} \sim \left(\frac{\epsilon}{\tau} \right)^{2\Delta[J_2, J_1]}, \quad (2.22)$$

⁷For more discussions about the correlation functions of BCC operators, see [47].

where $\Delta[J_2, J_1]$ is the conformal dimension of the operator $\mathcal{O}_{J_1 J_2}$.

The simplest setup is the following. We consider the Poincaré AdS₃ bulk solution with metric

$$ds^2 = \frac{dz^2 + dx_0^2 + dx_1^2}{z^2} \quad (2.23)$$

and two (tensionless) EOW branes

$$x_0^2 + x_1^2 + z^2 = b^2, \quad x_1 = a \equiv b \cos(\eta), \quad 0 < \eta < \frac{\pi}{2}. \quad (2.24)$$

The setup is illustrated in Figure 2 and 3. At the AdS boundary, these two EOW branes

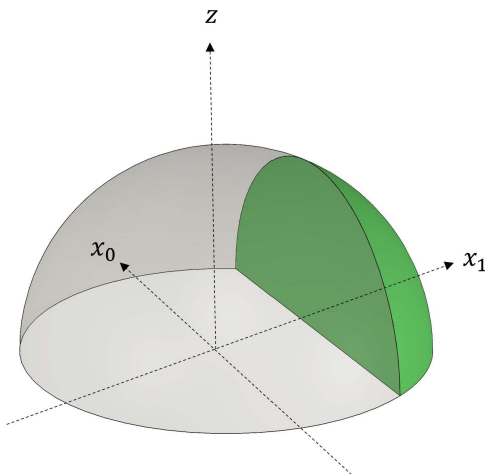


Figure 2: A simple gravity solution dual to the two-point correlation function of BCC operators. The shaded green region represents the bulk dual, bounded by two EOW branes and the AdS boundary.

intersect at $x_0 = \pm\tau_0$, $\tau_0 = b \sin(\eta)$. When η is small: $\eta \ll 1$, the leading contribution to the on-shell action can be approximated by the Weyl anomaly [48]

$$I \approx \frac{2\eta}{8\pi G_N} \log \frac{\epsilon}{b} - \left(-\frac{2 \tan(\eta)}{8\pi G_N} \log \frac{b}{\tau_0} \right) \approx \frac{\eta}{4\pi G_N} \log \frac{\epsilon}{\tau_0}, \quad (2.25)$$

leading to

$$Z = e^{-I} \approx \left(\frac{\epsilon}{\tau_0} \right)^{-2\Delta}, \quad \Delta = \frac{c}{12} \frac{\eta}{\pi}. \quad (2.26)$$

This result is equal to the inverse of the two-point function (2.22). In other words, the two-point function is dual to the Poincaré spacetime with this region excised. In the following sections, we will demonstrate that this phenomenon is quite common; specifically, correlation functions can be computed from the on-shell action of an excised geometry. For the two-point function of two bulk primaries, this result can be elucidated using the wedge construction of the conical geometry as previously discussed.

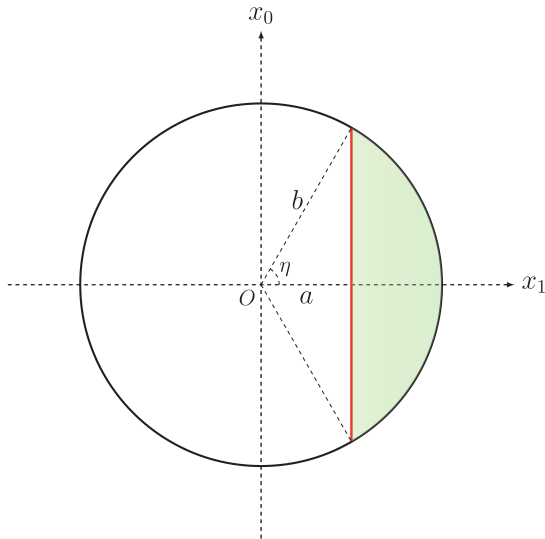


Figure 3: The bulk region in 2 is dual to a BCFT defined on the green-shaded region..

3 Cases study

In this section we construct the excised geometry on top of various AdS_3 solutions including the global AdS, Poincaré AdS and the BTZ black holes. Our construction strategy is as follows: we begin with the global AdS geometry described by the metric (2.13) and excise a wedge defined by⁸

$$-\eta < \theta < \eta, \quad \eta = \pi(1 - \alpha) = 4\pi G_N m. \quad (3.1)$$

As previously explained, this excised geometry is dual to a conical geometry, with the tip of the wedge corresponding to a massive particle situated at the center of the global AdS. Next, we perform a boost transformation (3.10). In this boosted frame, the trajectory of the particle (or the tip of the wedge) intersects the AdS boundaries at specific points, and the wedge now resembles a spindle. It is important to note that the boost transformation is an isometry of the global AdS spacetime, thus, we have constructed a global AdS spacetime with a spindle-like region excised, which is expected to be dual to the two-point function of two scalar primaries in a CFT defined in a finite interval. This resulting excised solution has already been considered in [27] as a holographic description of the Virasoro coherent state. To construct other excised geometries, we leverage the fact that there are no local degrees of freedom, allowing us to use the known coordinate transformation to transform one excised geometry into another. This strategy is quite standard, for example, it has been employed in the construction of shockwave geometries [49–53] caused by the backreaction of the massless particle. After constructing the excised geometries, we will compute the on-shell action either analytically or numerically to demonstrate that they indeed yield the

⁸In the construction of the conical geometry without boundaries in the bulk, we also need to glue the two edges of the wedge.

correct two-point functions. It is important to emphasize that we are performing an honest bulk calculation, meaning that we compute the on-shell actions of the excised geometries directly, rather than transforming them into other simple configurations as done in [27], which only matches our results at leading order.

3.1 Poincaré AdS₃

We begin by examining the simplest case: the excised Poincaré AdS₃, where all computations can be performed exactly. Given the metrics (2.13) and (2.23) of the global AdS₃ and the Poincaré AdS₃, we make the following identifications:

$$\begin{aligned}
\sqrt{r^2 + 1} \cosh \tau &= \cosh \beta \frac{z^2 + x_1^2 + x_0^2 + 1}{2z} - \sinh \beta \frac{x_0}{z}, \\
r \cos \theta &= -\sinh \beta \frac{z^2 + x_1^2 + x_0^2 + 1}{2z} + \cosh \beta \frac{x_0}{z}, \\
r \sin \theta &= \frac{x_1}{z}, \\
\sqrt{r^2 + 1} \sinh \tau &= \frac{z^2 + x_1^2 + x_0^2 - 1}{2z}.
\end{aligned} \tag{3.2}$$

It should be pointed out that when the boost parameter $\beta = 0$, the transformations (3.2) reduce to the standard coordinate transformations between global AdS₃ and Poincaré AdS₃. These identifications imply that the trajectory of a static particle in the global AdS₃ maps to a circle described by

$$(x_0 - \coth \beta)^2 + z^2 = \frac{1}{\sinh^2 \beta}, \quad x_1 = 0, \tag{3.3}$$

which intersects the AdS asymptotic boundary at the following two points

$$x_{0,a}, x_{0,b} = \coth \frac{\beta}{2}, \tanh \frac{\beta}{2}. \tag{3.4}$$

Meanwhile, the edges of the wedge, $\theta = \pm\eta$, are mapped into circles on a sphere defined by

$$\Sigma_{1,2} : (x_0 - \coth \beta)^2 + \left(x_1 \pm \frac{1}{\sinh \beta \tan \eta} \right)^2 + z^2 = \frac{1}{\sin^2 \eta \sinh^2 \beta}, \tag{3.5}$$

which represent the profiles of the tensionless EOW branes in Poincaré AdS₃. Notably, the intersection of these surfaces is precisely the worldline given in (3.3). According to AdS/BCFT correspondence, the wedge $\Sigma_1 \cap \Sigma_2$ is dual to a BCFT defined on $\partial\Sigma_1 \cap \partial\Sigma_2$, as illustrated in Figure 4.

The on-shell action (2.9) of this excised geometry has been computed in [27] and is also reproduced in Appendix A. Here, we provide some comments on this computation. The on-shell action in the total Poincaré AdS₃ is zero, as it corresponds to the vacuum state of

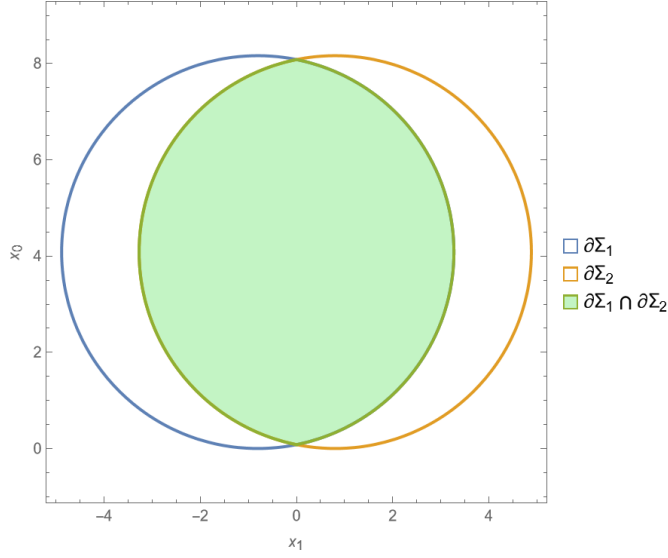


Figure 4: Boundary region dual to the bulk wedge in Poincaré AdS₃.

a CFT defined in the complex plane. Therefore, the on-shell action of the excised Poincaré geometry is equal to $-I_{\text{gravity},W}$. As explained in Section 2, the matter term cancels with the Hayward term associated with $\partial\Sigma_1 \cap \partial\Sigma_2$. The other two Hayward terms related to $\partial\Sigma_i \cap \partial\text{AdS}$ contribute only finite amounts. Consequently, the leading order contribution of (2.9) arises from the Weyl anomaly of the dual BCFT. The result is given by:

$$I_{\text{grav}} = -I_{\text{gravity},W} = -\frac{1}{8\pi G_N} \left[4\eta \log \frac{\epsilon}{b} - i (\text{Li}_2(e^{2i\eta}) - \text{Li}_2(e^{-2i\eta})) - 4\eta \right] \quad (3.6)$$

Recall the relation between the conformal dimension and the local mass of the particle is given by

$$\Delta = m(1 - 2G_N m) \approx m, \quad \text{when } G_N m \ll 1, \quad (3.7)$$

thus in the probe limit the partition function of the excised geometry exactly reproduces the two-point function

$$e^{-I_{\text{grav}}} \approx \frac{\epsilon^{2h+2\bar{h}}}{(u_{12})^{2h} (v_{12})^{2\bar{h}}} = \left(\frac{\epsilon}{x_{0,ab}} \right)^{2\Delta}. \quad (3.8)$$

where $h = \bar{h} = \frac{\Delta}{2}$ for scalar primary operators and the light-cone coordinate

$$u = x_1 + ix_0, \quad v = x_1 - ix_0 \quad (3.9)$$

is adopted.

3.2 Global AdS₃

In global AdS₃, the construction of the excised geometry is straightforward. We need only to perform the following boost:

$$\begin{aligned}
\sqrt{r_s^2 + 1} \cosh \tau_s &= \sqrt{r^2 + 1} \cosh (\tau - \tau_0) \cosh \beta - r \cos (\theta - \theta_0) \sinh \beta \\
r_s \cos \theta_s &= -\sqrt{r^2 + 1} \cosh (\tau - \tau_0) \sinh \beta + r \cos (\theta - \theta_0) \cosh \beta \\
r_s \sin \theta_s &= r \sin (\theta - \theta_0) \\
\sqrt{r_s^2 + 1} \sinh \tau_s &= \sqrt{r^2 + 1} \sinh (\tau - \tau_0)
\end{aligned} \tag{3.10}$$

where we have added a subscript s to denote the static frame for distinction. We can solve for the profile of the moving particle by setting $r = 0$ in the above transformations. The result is

$$\frac{r}{\sqrt{r^2 + 1}} = \tanh \beta \cosh (\tau - \tau_0), \quad \theta = \theta_0 + k\pi, k \in \mathbb{Z}. \tag{3.11}$$

which corresponds precisely to the intersection of two tensionless EOW branes with the profiles

$$\Sigma_{1,2} : \pm \tan \eta = \frac{r \sin (\theta - \theta_0)}{\sqrt{r^2 + 1} \cosh (\tau - \tau_0) \sinh \beta - r \cos (\theta - \theta_0) \cosh \beta}. \tag{3.12}$$

Without loss of generality, we set $k = \theta_0 = \tau_0 = 0$ in the following calculations. The two insertion points at the boundary are given by

$$\tau_1, \tau_2 = \pm \operatorname{arccosh} (\coth \beta) = \pm \tau_b, \quad \coth \beta \equiv \cosh \tau_b. \tag{3.13}$$

The relationship between the coordinate times defined along the worldline of the particle in the static and boost frame is

$$\tanh \tau_s = \cosh \beta \tanh \tau. \tag{3.14}$$

As shown in Figure 5, the excised wedge also takes the shape of a spindle, which is dual to a BCFT defined in the region $\partial\Sigma_1 \cap \partial\Sigma_2$ with

$$\partial\Sigma_{1,2} : \pm \tan \eta = \frac{\sin \theta}{\cosh \tau \sinh \beta - \cos \theta \cosh \beta}. \tag{3.15}$$

Similar to the previous case, the on-shell action of the entire global AdS₃ geometry and the Hayward terms only give finite contributions. The leading order contribution to the on-shell action arises from that in the wedge:

$$\begin{aligned}
I_{gravity,W} &= -\frac{1}{16\pi G_N} \int_{\mathcal{M}} \sqrt{g} (R + 2) - \frac{1}{8\pi G_N} \int_{\partial\mathcal{M}} \sqrt{h} (K - 1) \\
&= -\frac{1}{8\pi G_N} \int_{\partial\mathcal{M}} d^2x \left(r^2(\theta, \tau) + \frac{1}{2} \right),
\end{aligned} \tag{3.16}$$

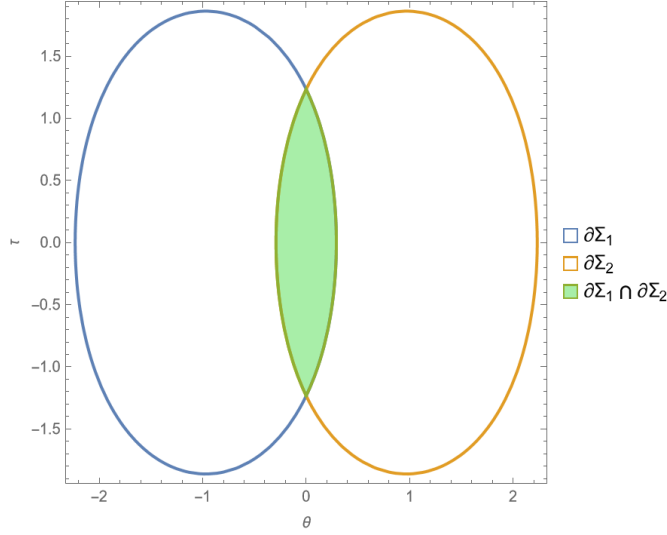


Figure 5: Boundary region dual to the bulk wedge in global AdS₃.

where $r(\theta, \tau)$ is a function of θ and τ determined from (3.12). To regularize the on-shell action, we choose a standard cutoff $r = \frac{1}{\epsilon}$. Then the integration domain $\partial\Sigma_1 \cap \partial\Sigma_2$ is explicitly given by:

$$-\theta(\tau) < \theta < \theta(\tau), \quad -\tau_c < \tau < \tau_c, \quad \tau_c = \operatorname{arccosh} \frac{\coth \beta}{\sqrt{1 + \epsilon^2}}. \quad (3.17)$$

Here, θ is a function of τ , determined from (3.12), yielding

$$\sin(\theta(\tau) - \Theta_0) = -\mu\sqrt{1 + \epsilon^2} \quad (3.18)$$

where we have introduced the following variables:

$$\cosh \beta \tan \eta = \tan \Theta_0, \quad \mu = \tanh \beta \sin \Theta_0 \cosh \tau, \quad (3.19)$$

for convenience. Since the wedge region is symmetric about $\theta = 0$ and $\tau = 0$, we will only consider the case $0 < \eta < \frac{\pi}{2}$, which implies $0 < \Theta_0 < \frac{\pi}{2}$ as β is assumed to be positive.

Substituting the explicit expression $r(\theta, \tau)$ into this integral gives

$$\begin{aligned} I_{gravity,W} &= -\frac{1}{8\pi G_N} \int_{-\tau_c}^{\tau_c} d\tau \int_0^{\theta(\tau)} d\theta \frac{(\cos \theta \cosh \beta \tan \eta - \sin \theta)^2 + (\tan \eta \sinh \beta \cosh \tau)^2}{(\cos \theta \cosh \beta \tan \eta - \sin \theta)^2 - (\tan \eta \sinh \beta \cosh \tau)^2} \\ &= -\frac{1}{8\pi G_N} \int_{-\tau_c}^{\tau_c} d\tau \int_0^{\theta(\tau)} d\theta \left[1 + \frac{2\mu^2}{\sin^2(\theta - \Theta_0) - \mu^2} \right] \\ &= -\frac{1}{8\pi G_N} \int_{-\tau_c}^{\tau_c} d\tau \left[\theta(\tau) + \frac{\mu \left(\log \frac{4(1-\mu^2)}{\epsilon^2} - \log \frac{\tan \Theta_0 + \frac{\mu}{\sqrt{1-\mu^2}}}{\tan \Theta_0 - \frac{\mu}{\sqrt{1-\mu^2}}} \right)}{\sqrt{1-\mu^2}} \right]. \end{aligned} \quad (3.20)$$

Note that the first term that appears in the integral is proportional to the area of the region $\partial\Sigma_1 \cap \partial\Sigma_2$, corresponding to the vacuum energy of the bulk wedge region. The second term plays a role similar to that in the case of the Poincaré AdS solution, contributing to the Weyl anomaly of the BCFT. The integral is too complicated to evaluate analytically. A numerical result is shown in Figure 6. We observe a linear dependence with respect to the angle η when η is small. A similar linear dependence is also observed in the case of Poincaré AdS solution. Motivated by these facts, to have some analytic understanding of the integral, we compute this integral perturbatively, order by order with respect to the deficit angle η . Expanding the integrand to the leading order of η gives

$$\eta \left(\cosh \beta - \sqrt{1 + \epsilon^2} \sinh \beta \cosh \tau \right) - \eta \sinh \beta \left(\log \frac{\epsilon^2}{4} + \log \frac{\coth \beta + \cosh \tau}{\coth \beta - \cosh \tau} \right) \cosh \tau. \quad (3.21)$$

and evaluating the resulting integral over τ gives the leading result of (3.20):

$$-\frac{1}{8\pi G_N} \left[-2\eta \log \frac{\epsilon^2}{4 \sin \frac{w_{12}}{2} \sin \frac{\bar{w}_{12}}{2}} - 2\eta \left(1 + \cosh \beta \log \left(\coth \frac{\beta}{2} \right) \right) \right] \quad (3.22)$$

where the light-cone coordinates have been introduced

$$w_1 = \theta_1 + i\tau_1 = i\tau_b, \quad w_2 = \theta_2 + i\tau_2 = -i\tau_b. \quad (3.23)$$

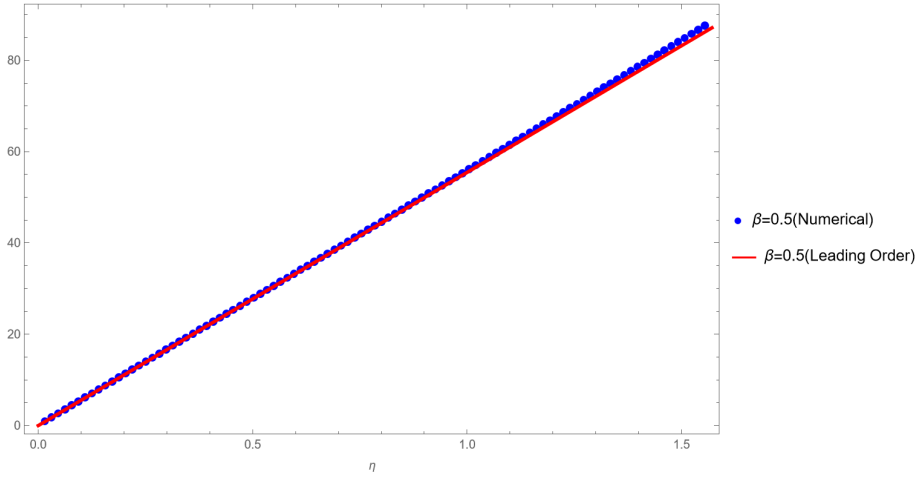


Figure 6: Numerical result of the integral in global AdS₃ when $\beta = 0.5, \epsilon = 10^{-6}$.

As shown in the Figure 6, the analytical result at leading order is consistent with the numerical result when β or η is small. Once we include the next order corrections, the deviation approaches zero as shown in Appendix C for β and η in a very large domain. Therefore, we conclude that the partition function is given by:

$$I_{grav} = -I_{gravity,W} \approx m \log \frac{\epsilon^2}{4 \sin \frac{w_{12}}{2} \sin \frac{\bar{w}_{12}}{2}} + m \left(1 + \cosh \beta \log \left(\coth \frac{\beta}{2} \right) \right) \quad (3.24)$$

which implies

$$\frac{e^{-I_{grav}}}{e^{-I_{grav,vacuum}}} \approx \frac{\epsilon^{2(h+\bar{h})}}{\left(2 \sin \frac{w_{12}}{2}\right)^{2h} \times \left(2 \sin \frac{\bar{w}_{12}}{2}\right)^{2\bar{h}}} \quad (3.25)$$

with $h = \bar{h} = \frac{m}{2}$ for scalar primary operators in the probe limit. It precisely reproduces the two-point function in a CFT defined on a finite circle.

3.3 BTZ

Finally, let us construct the excised BTZ geometry. The BTZ geometry [54, 55] can be described by the metric

$$ds^2 = \frac{f(z)d\tau^2}{z^2} + \frac{dz^2}{f(z)z^2} + \frac{dx^2}{z^2}, \quad f(z) = 1 - \frac{z^2}{z_H^2}, \quad \tau \sim \tau + 2\pi z_H. \quad (3.26)$$

Assuming rotational symmetry in its trajectory, the geodesic equation in the BTZ geometry can be solved as

$$z(\tau) = z_H \sqrt{1 - \left(1 - \frac{z_0^2}{z_H^2}\right) \left(1 + \tan^2 \frac{\tau - \tau_0}{z_H}\right)} \quad (3.27)$$

where τ_0 and z_0 are two integral constants. Below, we will obtain this by using our aforementioned strategy as the intersection of two tensionless EOW branes in the boosted frame. Recalling that the coordinates (τ, z, x) are related to the embedding coordinates via

$$\begin{aligned} X_0 &= \frac{z_H}{z} \cosh \frac{x}{z_H}, & X_1 &= \sqrt{\frac{z_H^2}{z^2} - 1} \cos \frac{\tau}{z_H}, \\ X_2 &= \frac{z_H}{z} \sinh \frac{x}{z_H}, & X_3 &= \sqrt{\frac{z_H^2}{z^2} - 1} \sin \frac{\tau}{z_H}, \end{aligned} \quad (3.28)$$

we find that the boosted frame should be defined by

$$\begin{aligned} \sqrt{r^2 + 1} \cosh \tilde{\tau} &= \frac{z_H}{z} \cosh \frac{x}{z_H} \cosh \beta - \sqrt{\frac{z_H^2}{z^2} - 1} \cos \frac{\tau}{z_H} \sinh \beta, \\ r \cos \theta &= -\frac{z_H}{z} \cosh \frac{x}{z_H} \sinh \beta + \sqrt{\frac{z_H^2}{z^2} - 1} \cos \frac{\tau}{z_H} \cosh \beta, \\ r \sin \theta &= \frac{z_H}{z} \sinh \frac{x}{z_H}, \\ \sqrt{r^2 + 1} \sinh \tilde{\tau} &= \sqrt{\frac{z_H^2}{z^2} - 1} \sin \frac{\tau}{z_H}, \end{aligned} \quad (3.29)$$

where $\tilde{\tau}$ has been introduced to denote the time in the global AdS₃ for distinction. It should be pointed out that a similar relation was used in [33, 56] for studying the

entanglement entropy of the (rotating) BTZ black hole perturbed by a massive backreacted free-falling particle. The relations (3.29) imply that the surfaces $\theta = \pm\eta$ are mapped into two EOW brane profiles

$$\Sigma_{1,2} : \pm \tan \eta = \frac{\sinh \frac{x}{z_H}}{-\sinh \beta \cosh \frac{x}{z_H} + \sqrt{1 - \frac{z^2}{z_H^2}} \cos \frac{\tau}{z_H} \cosh \beta}. \quad (3.30)$$

The intersection is given by

$$z = z_H \sqrt{1 - \tanh^2 \beta \left(1 + \tan^2 \frac{\tau}{z_H}\right)}, \quad x = 0, \quad (3.31)$$

which coincides with the geodesic (3.27), up to the following identification

$$z_0 = \frac{z_H}{\cosh \beta}, \quad \tau_0 = 0. \quad (3.32)$$

Note that z_0 is also the deepest position of this geodesic in the bulk, which is outside the horizon. The transformations (3.29) also imply that the two endpoints of this geodesic are at

$$\tau_{1,2} = \pm z_H \tau_b, \quad x_{1,2} = 0, \quad \tanh \beta \equiv \cos \tau_b, \quad (3.33)$$

and the relation between the coordinate time along the trajectory in the boosted frame and the static frame is

$$\tanh \tilde{\tau} = \sinh \beta \tan \frac{\tau}{z_H}. \quad (3.34)$$

As shown in Figure 7, the wedge in the boosted frame still has the shape of a spindle, but the EOW branes have two possible configurations depending on the value of the combination $\mathcal{G} = \tan \eta \sinh \beta$. When $0 < \mathcal{G} \leq 1$, the surfaces $\Sigma_{1,2}$ terminate at the event horizon $z = z_H$; whereas, when $\mathcal{G} > 1$, the surfaces $\Sigma_{1,2}$ will turn around before reaching the horizon, resembling the behavior in global AdS₃. In either case, the dual BCFT is defined in $\partial\Sigma_1 \cap \partial\Sigma_2$ with

$$\partial\Sigma_{1,2} : \pm \tan \eta = \frac{\sinh \frac{x}{z_H}}{-\sinh \beta \cosh \frac{x}{z_H} + \cos \frac{\tau}{z_H} \cosh \beta}. \quad (3.35)$$

on-shell action: $\mathcal{G} < 1$

First, let us consider the case of $\mathcal{G} < 1$. As explained before, the leading contribution to the on-shell action comes from that in the wedge:

$$\begin{aligned} I_{gravity,W} &= -\frac{1}{16\pi G_N} \int_{\mathcal{M}} \sqrt{g} (R + 2) - \frac{1}{8\pi G_N} \int_{\partial\mathcal{M}} \sqrt{h} (K - 1) \\ &= \frac{1}{4\pi G_N} \int_{\partial\mathcal{M}} d^2x \left(\frac{1}{2\epsilon^2} - \frac{1}{2z^2(\tau, x)} \right) - \frac{1}{8\pi G_N} \int_{\partial\mathcal{M}} d^2x \left(\frac{1}{\epsilon^2} - \frac{1}{2z_H^2} \right) \\ &= -\frac{1}{8\pi G_N} \int_{\partial\mathcal{M}} d^2x \left(\frac{1}{z^2(\tau, x)} - \frac{1}{2z_H^2} \right). \end{aligned} \quad (3.36)$$

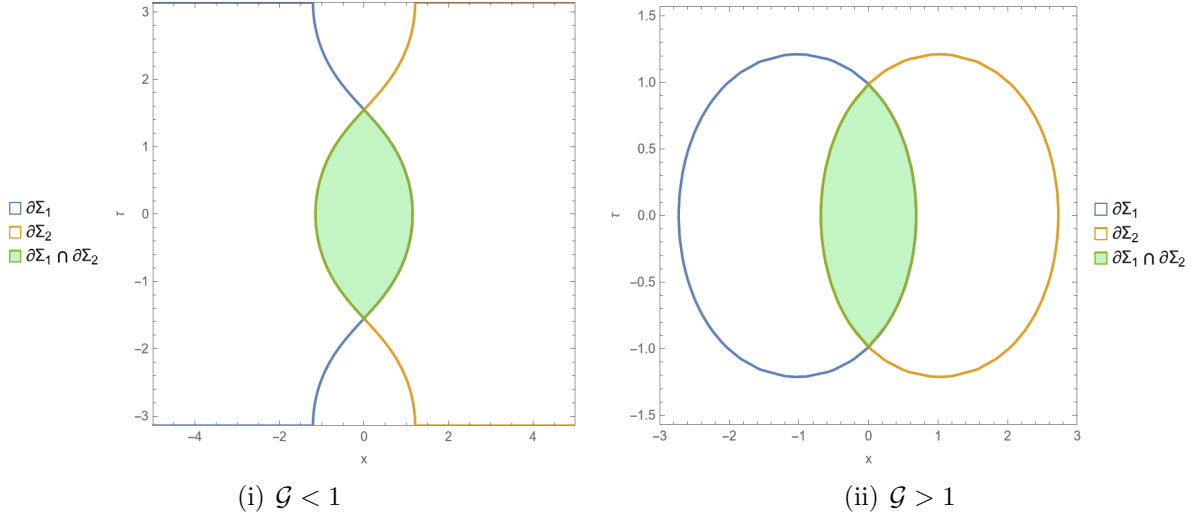


Figure 7: Boundary region dual to the bulk wedge in BTZ black hole

where z is a function of x and τ solved from (3.30). Then the integration domain $\partial\Sigma_1 \cap \partial\Sigma_2$ is explicitly given by:

$$-x(\tau) < x < x(\tau), \quad -\tau_c < \tau < \tau_c, \quad (3.37)$$

$$x(\tau) + x_0 = z_H \sinh^{-1} \left(\mu \sqrt{1 - \frac{\epsilon^2}{z_H^2}} \right), \quad \tau_c = z_H \arccos \frac{\tanh \beta}{\sqrt{1 - \frac{\epsilon^2}{z_H^2}}}, \quad (3.38)$$

where we have chosen a cutoff $z = \epsilon$ for regularization and introduced the following convenient variables:

$$\tanh \frac{x_0}{z_H} = \mathcal{G} \equiv \tan \eta \sinh \beta, \quad \mu = \sinh \frac{x_0}{z_H} \coth \beta \cos \frac{\tau}{z_H}. \quad (3.39)$$

Substituting the explicit expression of $z(\tau, x)$ into the above integral, we obtain

$$\begin{aligned} I_{gravity, W} &= -\frac{1}{8\pi G_N z_H^2} \int_{-\tau_c}^{\tau_c} d\tau \int_0^{x(\tau)} \left(-1 + \frac{2\mu^2}{\mu^2 - \sinh^2 \frac{x+x_0}{z_H}} \right) dx \\ &= -\frac{1}{8\pi G_N z_H} \int_{-\tau_c}^{\tau_c} d\tau \left[-\frac{x(\tau)}{z_H} + \frac{\mu \left(\log \frac{4z_H^2(1+\mu^2)}{\epsilon^2} - \log \frac{\frac{\mu}{\sqrt{\mu^2+1}} + \tanh \frac{x_0}{z_H}}{\frac{\mu}{\sqrt{\mu^2+1}} - \tanh \frac{x_0}{z_H}} \right)}{\sqrt{\mu^2+1}} \right]. \quad (3.40) \end{aligned}$$

To tackle this integral, we employ our previous perturbative strategy. When η is small and the parameter β satisfies $\beta < \sinh^{-1}(\cot \eta)$, we can expand the integrand in terms of η , at the first order yielding

$$\eta \left(\sinh \beta - \sqrt{1 - \frac{\epsilon^2}{z_H^2}} \cos \frac{\tau}{z_H} \cosh \beta \right) + \eta \cosh \beta \left(\log \frac{4z_H^2}{\epsilon^2} - \log \frac{\cos \frac{\tau}{z_H} + \tanh \beta}{\cos \frac{\tau}{z_H} - \tanh \beta} \right) \cos \frac{\tau}{z_H}.$$

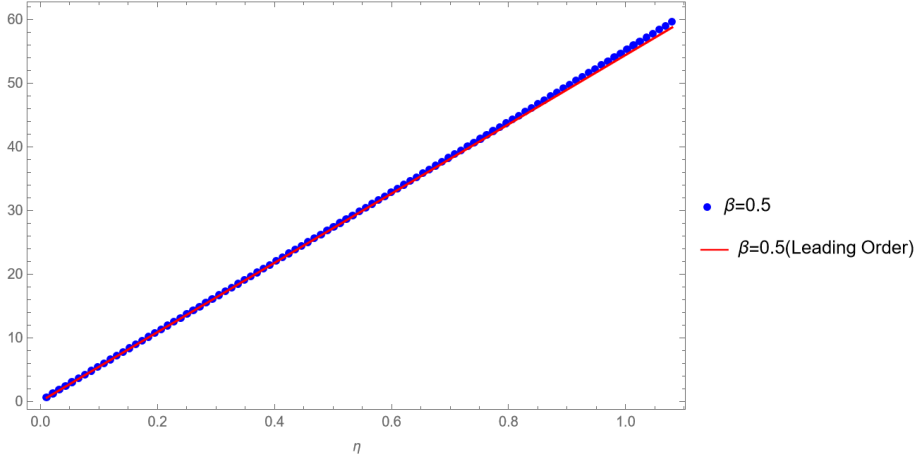


Figure 8: Numerical result and analytical result at leading order perturbation when $\mathcal{G} < 1$.

Now, this integral can be analytically evaluated, and the result is

$$I_{gravity,W} \approx m \left(\log \frac{\epsilon^2}{4z_H^2 \sinh \frac{w_{12}}{2z_H} \sinh \frac{\bar{w}_{12}}{2z_H}} + 1 + \cos^{-1}(\tanh \beta) \sinh \beta \right) = -I_{grav}, \quad (3.41)$$

where we have used identity $\sinh \frac{w_{12}}{2z_H} \sinh \frac{\bar{w}_{12}}{2z_H} = \text{sech}^2 \beta$, $\eta = 4\pi G_N m$, and introduced light-cone coordinates

$$w_1 = x_1 + i\tau_1 = iz_H \tau_b, \quad w_2 = x_2 + i\tau_2 = -iz_H \tau_b. \quad (3.42)$$

As illustrated in Figure 8, when $\eta < 1$, the numerical result is almost linear to η and nearly coincides with the analytical result at leading order perturbation. Once the deficit angle η is increased, the contribution of high-order perturbation should be included so that the deviation will be smoothed, as illustrated in the appendix C.

Since the second term in the above result is nearly equal to the boundary area of the BCFT region, if we only consider the leading order contribution, the partition function of the excised geometry exactly reproduces the two-point function in BTZ black hole

$$\frac{e^{-I_{grav}}}{e^{-I_{grav,vacuum}}} \approx \frac{\epsilon^{2h+2\bar{h}}}{\left(2z_H \sinh \frac{w_{12}}{2z_H}\right)^{2h} \left(2z_H \sinh \frac{\bar{w}_{12}}{2z_H}\right)^{2\bar{h}}} \quad (3.43)$$

with $h = \bar{h} = \frac{\Delta}{2}$ for scalar primary operators in the probe limit. It precisely reproduces the two-point function in a CFT in a thermal state.

on-shell action: $\mathcal{G} = 1$

In this case, the integral (3.36) is dramatically simplified to

$$\begin{aligned}
I_{gravity,W} &= -\frac{1}{8\pi G_N z_H} \int_{-\tau_c}^{\tau_c} d\tau \left[\frac{x(\tau)}{z_H} + \log(\mu^2 - 1) - \log \frac{\mu^2 \epsilon^2}{z_H^2} \right] \\
&= -\frac{1}{8\pi G_N z_H} \int_{-\tau_c}^{\tau_c} d\tau \left[-\log \frac{\epsilon^2}{z_H^2} + \log \frac{\mu^2 - 1}{\mu} \right] \\
&= -\frac{1}{8\pi G_N} \left[-2\eta \log \frac{\epsilon^2}{z_H^2} + \mathcal{F} \left(\frac{\tau_c}{z_H} \right) \right], \tag{3.44}
\end{aligned}$$

where we have used the following expressions:

$$\begin{aligned}
x(\tau) &= z_H \log \left(\mu \sqrt{1 - \frac{\epsilon^2}{z_H^2}} \right), \quad \mu = \coth \beta \cos \frac{\tau}{z_H}, \\
\frac{\tau_c}{z_H} &= \arccos \left(\frac{\cos \eta}{\sqrt{1 - \frac{\epsilon^2}{z_H^2}}} \right). \tag{3.45}
\end{aligned}$$

Here, the complicated function \mathcal{F} is given by ⁹

$$\begin{aligned}
\mathcal{F} \left(\frac{\tau_c}{z_H} \right) &= \int_{-\frac{\tau_c}{z_H}}^{\frac{\tau_c}{z_H}} \log(\cos x) dx + \int_{-\frac{\tau_c}{z_H}}^{\frac{\tau_c}{z_H}} \log(1 - \cos^2 \eta \sec^2 x) dx - \frac{2\tau_c}{z_H} \log(\tanh \beta) \\
&= -2\eta \log(2 \cos \eta) + \frac{i(2\text{Li}_2(e^{2i\eta}) - 2\text{Li}_2(e^{-2i\eta}) + \text{Li}_2(e^{4i\eta}) - \text{Li}_2(e^{-4i\eta}))}{4}. \tag{3.46}
\end{aligned}$$

As shown in Figure 9, this analytical result matches the numerical result very well. When η is small, we find that in the leading order the on-shell action is

$$\begin{aligned}
I_{grav} &= -I_{gravity,W} \approx -m \left(\log \frac{\epsilon^2}{4z_H^2 \eta^2} + 2 \right) \approx -m \left(\log \frac{\epsilon^2}{4z_H^2 \sin^2(\eta)} + 2 \right) \\
&\approx -m \left(\log \frac{\epsilon^2}{4z_H^2 \sinh \frac{w_{12}}{2z_H} \sinh \frac{\bar{w}_{12}}{2z_H}} + 2 \right). \tag{3.47}
\end{aligned}$$

This shows that, up to a redefinition of the cutoff surface, the partition function $e^{-I_{grav}} \sim e^{I_{gravity,W}}$ exactly reproduces the two-point function in BTZ geometry.

⁹Here, we have used the following result: $g(x) \equiv \int \log(\cos x) dx = -\frac{ix^2}{2} - x \log 2 - \frac{\text{Li}_2(-e^{2ix})}{2i}$

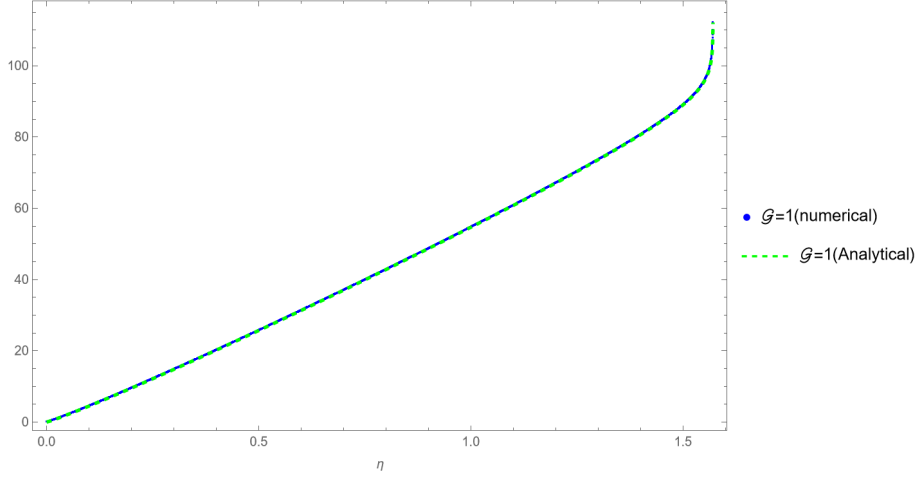


Figure 9: Comparison between the numerical result and analytical result when $\mathcal{G} = 1$.

on-shell action: $\mathcal{G} > 1$

In the end, let us consider the case of $\mathcal{G} > 1$. The integral (3.36) is explicitly given by

$$\begin{aligned}
I_{gravity,W} &= -\frac{1}{8\pi G_N z_H^2} \int_{-\tau_c}^{\tau_c} d\tau \int_0^{x(\tau)} \left(-1 + \frac{2\mu^2}{\mu^2 - \cosh^2 \frac{x+x_0}{z_H}} \right) dx \\
&= -\frac{1}{8\pi G_N z_H} \int_{-\tau_c}^{\tau_c} d\tau \left[\frac{-x(\tau)}{z_H} + \frac{\mu \left(\log \frac{4z_H^2(\mu^2-1)}{\epsilon^2} - \log \frac{\frac{\sqrt{\mu^2-1} + \tanh \frac{x_0}{z_H}}{\mu}}{\frac{\sqrt{\mu^2-1} - \tanh \frac{x_0}{z_H}}{\mu}} \right)}{\sqrt{\mu^2-1}} \right], \quad (3.48)
\end{aligned}$$

where we have adopted the following conventions

$$x(\tau) + x_0 = z_H \cosh^{-1} \left(\mu \sqrt{1 - \frac{\epsilon^2}{z_H^2}} \right), \quad (3.49)$$

$$\coth \frac{x_0}{z_H} = \mathcal{G}, \quad \mu = \cosh \frac{x_0}{z_H} \coth \beta \cos \frac{\tau}{z_H}. \quad (3.50)$$

Following our previous discussion, we find that in the leading order of η , the on-shell action is

$$I_{grav} = -I_{gravity,W} \approx -2h \log \frac{\epsilon^2}{2z_H \sinh \frac{w_{12}}{2z_H} \times 2z_H \sinh \frac{\bar{w}_{12}}{2z_H}} \quad (3.51)$$

as desired.

4 Backreacted geometries

Instead of employing the wedge construction, in AdS_3 we can directly construct the backreacted geometries by following a similar approach proposed in [28, 33], which will be explained below. We begin with the metric (2.2) of the conical AdS,

$$ds^2 = (r^2 + \alpha^2)d\tau^2 + \frac{dr^2}{r^2 + \alpha^2} + r^2d\theta^2, \quad (4.1)$$

which we recall here for convenience. To construct the backreacted geometry corresponding to a two-point function in the Poincaré AdS, we perform the following coordinate transformation

$$\begin{aligned} \sqrt{r^2 + 1} \cosh \tau &= \cosh \beta \frac{z^2 + x_1^2 + x_0^2 + 1}{2z} - \sinh \beta \frac{x_0}{z} \\ r \cos \theta &= -\sinh \beta \frac{z^2 + x_1^2 + x_0^2 + 1}{2z} + \cosh \beta \frac{x_0}{z} \\ r \sin \theta &= \frac{x_1}{z} \\ \sqrt{r^2 + 1} \sinh \tau &= \frac{z^2 + x_1^2 + x_0^2 - 1}{2z}, \end{aligned} \quad (4.2)$$

which is the same as the one-parameter transformations introduced in [28, 33], which facilitate the construction of a holographic dual description for a local quench model up to a shift in the x_0 direction. The resulting geometry is very complicated, corresponding to a Poincaré spacetime deformed by the backreaction of a local excitation. We will refer to this backreacted geometry as the “deformed geometry”. It is important to emphasize that we previously used these transformations (3.2) in the wedge construction, but here we use them differently. In the earlier case, the coordinates (r, τ, θ) described the global AdS_3 with metric (2.13) and these transformations mapped the global AdS spacetime to the Poincaré AdS spacetime. In the current context, the meaning of transformations (4.2) is more intricate than they appear. As noted in [21], these transformations represent a combination of a GtP transformation and a special conformal transformation. Moreover, while the deformed Poincaré solution derived from these transformations is very complicated, the on-shell action of this backreacted geometry can be computed quite straightforwardly. The computation reduces to a surface integral over the non-standard cut-off surface at $z = \epsilon$, involving the non-trivial determinant of the induced metric:

$$\sqrt{h} = \frac{1}{\epsilon^2} - \frac{2(1 - \alpha^2)}{\sinh^2 \beta \left(x_1^2 + \left(x_0 - \tanh \frac{\beta}{2} \right)^2 \right) \left(x_1^2 + \left(x_0 - \coth \frac{\beta}{2} \right)^2 \right)}. \quad (4.3)$$

Similarly, other backreacted geometries can be constructed by applying the coordinate transformations (3.10) and (3.29).

Before proceeding with the calculation of the on-shell action in this background geometry, we outline here also the essential geometric setup required for the calculation of the on-shell action in the FG gauge for future use, which takes the general form

$$ds_{\text{FG}}^2 = \frac{dz_f^2 + (du_f + z_f^2 \bar{\mathcal{L}}(v_f) dv_f) (dv_f + z_f^2 \mathcal{L}(u_f) du_f)}{z_f^2}. \quad (4.4)$$

Different solutions are characterized by the functions $\mathcal{L}(u_f)$ and $\bar{\mathcal{L}}(v_f)$, which are related to the expectation value of the energy-stress tensor via [57]:

$$\mathcal{L}(u_f) = -\frac{6}{c} \langle T(u_f) \rangle, \quad \bar{\mathcal{L}}(v_f) = -\frac{6}{c} \langle \bar{T}(v_f) \rangle. \quad (4.5)$$

For instance, for the conical AdS geometry, the corresponding functions are

$$\mathcal{L} = \frac{\alpha^2}{4}, \quad \bar{\mathcal{L}} = \frac{\alpha^2}{4}. \quad (4.6)$$

To derive $\mathcal{L}(\bar{\mathcal{L}})$ for other deformed geometries, one can either solve the FG gauge directly by making an ansatz in the form of an expansion with respect to the AdS radial coordinate [28] or use the transformation rule of the energy-stress tensor

$$\langle T(u) \rangle = \left(\frac{dw}{du} \right)^2 \langle T(w) \rangle + \frac{c}{12} \text{Sch}(w, u) \quad (4.7)$$

where the Schwarzian derivative is defined as

$$\text{Sch}(w, u) = \frac{w'''(u)}{w'(u)} - \frac{3(w''(u))^2}{2(w'(u))^2}, \quad (4.8)$$

with u, w being the light-cone coordinates at the AdS boundary. The second method can also tell us the relationship between the CFT states that are dual to the bulk solutions before and after transformations. For example, as we approach the AdS boundary, the transformations (4.2) reduce to

$$u = \frac{\sinh \frac{\beta}{2} + e^w \cosh \frac{\beta}{2}}{\cosh \frac{\beta}{2} + e^w \sinh \frac{\beta}{2}}, \quad v = \frac{\sinh \frac{\beta}{2} + e^{\bar{w}} \cosh \frac{\beta}{2}}{\cosh \frac{\beta}{2} + e^{\bar{w}} \sinh \frac{\beta}{2}}, \quad (4.9)$$

where the conventions of the light-cone coordinates are

$$w = \tau + i\theta, \quad u = x_0 + ix_1. \quad (4.10)$$

Substituting into (4.7) and (4.6) yields

$$\mathcal{L}(u) = -\frac{1 - \alpha^2}{4} \frac{u_{ab}^2}{(u - u_a)^2 (u - u_b)^2}, \quad (4.11)$$

where

$$u_a \equiv \coth \frac{\beta}{2}, \quad u_b \equiv \tanh \frac{\beta}{2}. \quad (4.12)$$

Notably, since $\cosh^2(\frac{\beta}{2}) - \sinh^2(\frac{\beta}{2}) = 1$, the transformation (4.9) can be interpreted as a compound transformation $u = f_\beta(e^w)$, where f_β is a Möbius transformation. Recall that conical AdS geometry is dual to a primary state; thus the transformation (4.9) implies that the CFT state corresponding to the deformed Poincaré geometry is given by

$$|h\rangle \xrightarrow{e^w} \mathcal{O}(0)|\Omega\rangle \xrightarrow{\text{Möbius}} \mathcal{O}(u_a)|\Omega\rangle, \quad u_a = \tanh \frac{\beta}{2}. \quad (4.13)$$

Similarly, we find that FG gauges of the deformed global AdS and deformed BTZ are characterized by¹⁰

$$\mathcal{L}(u_{\text{global}}) = \frac{1}{4} - \frac{1 - \alpha^2}{4(\cosh \beta - \sinh \beta \cosh u_{\text{global}})^2}, \quad (4.14)$$

$$\mathcal{L}(u_{\text{BTZ}}) = -\frac{1}{4z_H^2} - \frac{1 - \alpha^2}{4z_H^2(\cosh \beta \cosh(u_{\text{BTZ}}/z_H) - \sinh \beta)^2}. \quad (4.15)$$

4.1 The on-shell action

After outlining our general approach, we present the calculation of the on-shell actions for the deformed geometries derived from the transformation, as well as those in their FG gauge. Specifically, we compute the gravitational action defined by (2.3), under the assumption that the matter term is canceled by the gravitational contribution associated with the conical singularity. We will demonstrate that the on-shell actions of the former are directly related to the correlation functions, whereas the on-shell actions of the latter are not. This distinction represents one of the key results of this paper.

On-shell action of deformed Poincaré AdS

We begin with the deformed Poincaré AdS geometry. As mentioned above, we apply the above transformation (4.2) into conical AdS₃, it's straightforward to show the determinant is invariant under the transformation

$$\sqrt{g} = \frac{1}{z^3} \quad (4.16)$$

¹⁰In the deformed BTZ, in order to obtain the correct result, the light-cone coordinate should be chosen as $u_{\text{BTZ}} = x + i\tau_{\text{BTZ}}$ due to the non-standard transformation we have chosen.

and the determinant of the induced metric on a naive cutoff surface is given by (4.3). So the on-shell action in this deformed Poincaré patch is given by

$$\begin{aligned}
I^{BR} &= -\frac{1}{16\pi G_N} \int_{\mathcal{M}} \sqrt{g} (R+2) - \frac{1}{8\pi G_N} \int_{\partial\mathcal{M}} \sqrt{h} (K-1) + m \int_{\Gamma} \sqrt{\gamma} \\
&= \frac{1-\alpha^2 |u_{ab}|^2}{4\pi G_N} \frac{1}{4} \int_{\partial\mathcal{M}} \frac{\sqrt{g^{(0)}} du dv}{|u-u_a|^2 |u-u_b|^2} \\
&= \frac{h |u_{ab}|^2}{\pi} \int_{\partial\mathcal{M}} \frac{\sqrt{g^{(0)}} du dv}{|u-u_a|^2 |u-u_b|^2}
\end{aligned} \tag{4.17}$$

where the boundary metric

$$ds^2 = g_{ij}^{(0)} dx^i dx^j = dudv \tag{4.18}$$

have been introduced. The detail of this integral can be found in the appendix B. We present the final result as follows

$$I^{BR} = \frac{h |u_{ab}|^2}{\pi} \times \frac{2\pi}{|u_{ab}|^2} \log \frac{u_{ab} v_{ab}}{\epsilon^2} = 4h \log \frac{|u_{ab}|}{\epsilon} \tag{4.19}$$

which indicates the partition function defined in the constructed solution exactly reproduces the two-point correlation function

$$e^{-I^{BR}} = \frac{\epsilon^{2(h+\bar{h})}}{(u_{ab})^{2h} (v_{ab})^{2\bar{h}}} = \left(\frac{\epsilon}{|u_{ab}|} \right)^{2\Delta}. \tag{4.20}$$

where $h = \bar{h} = \frac{\Delta}{2}$ for scalar primary operators.

While in its FG patch, where a wall at which the determinant of the FG expansion becomes degenerate always exists in the bulk and its expression is determined by

$$z_f = z_w, \quad z_w^{-4} = \mathcal{L}(u_f) \bar{\mathcal{L}}(v_f). \tag{4.21}$$

The on-shell action takes the following form

$$\begin{aligned}
I_{\text{FG}}^{BR} &= \frac{c}{6\pi} \int_{\partial\mathcal{M}} \sqrt{g^{(0)}} du_f dv_f \int_{\epsilon}^{z_w} \left(\frac{1}{z_f^3} - \mathcal{L}(u_f) \bar{\mathcal{L}}(v_f) z_f \right) dz_f - \frac{c}{12\pi} \int_{\partial\mathcal{M}} \sqrt{g^{(0)}} du_f dv_f \frac{1}{\epsilon^2} \\
&= -\frac{c}{6\pi} \int_{\partial\mathcal{M}} \sqrt{g^{(0)}} du_f dv_f \sqrt{\mathcal{L}(u_f) \bar{\mathcal{L}}(v_f)}
\end{aligned} \tag{4.22}$$

in general. In this case, substituting the (4.3) into above integral gives

$$I_{\text{FG}}^{BR} = -2h \log \frac{u_{ab} v_{ab}}{\epsilon^2} \tag{4.23}$$

which implies the partition function in FG patch gives the inverse of the two-point function. This can be interpreted as indicating that the FG coordinates cover only the region outside the following surface in deformed Poincaré AdS, given by

$$z^{-2} = \frac{u_{ab}v_{ab}(1-\alpha^2)}{(u-u_a)(u-u_b)(v-v_a)(v-v_b)} \quad (4.24)$$

which is the image of the wall, as showed in Figure 10. When $\beta \rightarrow 0$, this surface reduces to a conical surface $\frac{R}{z} = \sqrt{1-\alpha^2}$ as presented in [21]. It is straightforward to verify that

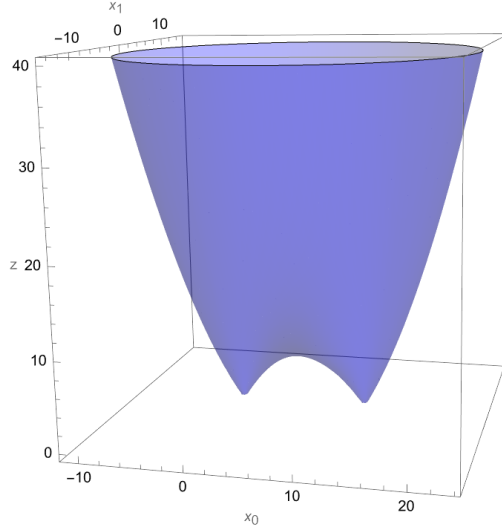


Figure 10: Image of the Wall in deformed Poincaré AdS.

the on-shell action computed in the region outside the image surface of the wall is identical to that in the FG coordinates:

$$I_{image,out}^{BR} = I_{FG}^{BR} \quad (4.25)$$

On-shell action of deformed global AdS

In deformed global AdS, the determinant is also invariant under the transformation

$$\sqrt{g} = r \quad (4.26)$$

and the determinant of the induced metric at a naive cutoff $r = \frac{1}{\epsilon}$ is given by

$$\begin{aligned} \sqrt{h} &= \frac{1}{\epsilon^2} + \frac{1}{2} \left(1 - \frac{1-\alpha^2}{\sinh^2 \beta (\cosh w - \coth \beta) (\cosh \bar{w} - \coth \beta)} \right) \\ &= \frac{1}{\epsilon^2} + \frac{1}{2} \left(1 - \frac{1-\alpha^2}{4} \frac{\sinh w_b \sinh \bar{w}_b}{\sinh \frac{w-w_b}{2} \sinh \frac{w+w_b}{2} \sinh \frac{\bar{w}-\bar{w}_b}{2} \sinh \frac{\bar{w}+\bar{w}_b}{2}} \right) \end{aligned} \quad (4.27)$$

where

$$\cosh w_b \equiv \coth \beta, \quad w_b = \tau_b. \quad (4.28)$$

In this case, the on-shell action defined in deformed global AdS is

$$\begin{aligned} I^{BR} &= -\frac{1}{16\pi G_N} \int_{\mathcal{M}} \sqrt{g} (R+2) - \frac{1}{8\pi G_N} \int_{\partial\mathcal{M}} \sqrt{h} (K-1) + m \int_{\Gamma} \sqrt{\gamma} \\ &= -\frac{1}{16\pi G_N} \int_{\partial\mathcal{M}} dwd\bar{w} \sqrt{g^{(0)}} \left(1 - \frac{1-\alpha^2}{4} \frac{\sinh w_b \sinh \bar{w}_b}{\sinh \frac{w-w_b}{2} \sinh \frac{w+w_b}{2} \sinh \frac{\bar{w}-\bar{w}_b}{2} \sinh \frac{\bar{w}+\bar{w}_b}{2}} \right) \\ &= -\frac{WT}{16\pi G_N} + \frac{h \sinh w_b \sinh \bar{w}_b}{4\pi} \int_{\partial\mathcal{M}} \frac{\sqrt{g^{(0)}} dwd\bar{w}}{\left| \sinh \frac{w-w_b}{2} \right|^2 \left| \sinh \frac{w+w_b}{2} \right|^2} \\ &= I_{\text{global, vacuum}} + 2h \log \frac{2 \sinh w_b \times 2 \sinh \bar{w}_b}{\epsilon^2} \end{aligned} \quad (4.29)$$

where $W = 2\pi$ represents the width of the boundary cylinder, T is the length of the boundary cylinder or the period along the Euclidean time τ direction. In the final step, we performed the transformation $u = e^w$, which maps an infinite cylinder onto the complex plane. This allows the integral to be evaluated as follows:

$$\int_{\partial\mathcal{M}} \frac{\sqrt{g^{(0)}} dwd\bar{w}}{\left| \sinh \frac{w-w_b}{2} \right|^2 \left| \sinh \frac{w+w_b}{2} \right|^2} = 16 |u_1| |u_2| \int_{\partial\mathcal{M}} \frac{\sqrt{g^{(0)}} dudv}{|u-u_1|^2 |u-u_2|^2} = \frac{32\pi |u_1| |u_2|}{|u_{12}|^2} \log \frac{u_{12} v_{12}}{(2\delta)^2}. \quad (4.30)$$

Recall that

$$\frac{4 |u_1| |u_2|}{|u_{12}|^2} = \frac{1}{\sinh \frac{w_{12}}{2} \sinh \frac{\bar{w}_{12}}{2}} = \frac{1}{\sinh w_b \sinh \bar{w}_b}, \quad w_{1,2} = \pm \tau_b \quad (4.31)$$

up to a redefinition of the cutoff

$$\frac{1}{\epsilon^2} = \frac{|u_1| |u_2|}{4\delta^2} = \frac{1}{4\delta^2}, \quad u_{1,2} = e^{\mp \tau_b}, \quad (4.32)$$

the above result is successfully reproduced, yielding the partition function as

$$\frac{e^{-I_{BR}}}{e^{-I_{\text{global, vacuum}}}} = \frac{\epsilon^{2h+2\bar{h}}}{(2 \sinh \frac{w_{12}}{2})^{2h} (2 \sinh \frac{\bar{w}_{12}}{2})^{2\bar{h}}} = \left(\frac{\epsilon^2}{2 \sinh \frac{w_{12}}{2} \times 2 \sinh \frac{\bar{w}_{12}}{2}} \right)^\Delta \quad (4.33)$$

with $h = \bar{h} = \frac{\Delta}{2}$ for scalar primary operators. The result matches the two-point function in global AdS up to an analytic continuation $\tau = it$, which arises from the different convention adopted here.

It is important to emphasize that the calculation above relies on the implicit assumption that the period T along the Euclidean time τ direction is either non-compact or much larger than the insertion points, $T \gg 2\tau_b$. This assumption allows us to neglect the boundary terms appearing in the integral (4.30), as detailed in Appendix B. Specifically,

if we assume the range of τ is $-\frac{T}{2} < \tau < \frac{T}{2}$, then the boundary cylinder is mapped to an annulus $e^{-\frac{T}{2}} < R < e^{\frac{T}{2}}$ in the complex plane. In evaluating the integral, we should include the following boundary term¹¹

$$2h \log \frac{\cosh T - \cosh(2\tau_b)}{\cosh T - 1}, \quad (4.34)$$

which is of constant order. Obviously, when $T \gg 2\tau_b$, its contribution can be neglected.

However, in the FG gauge, the on-shell action is no longer the negative of that (4.29) in deformed global AdS, as shown below. In the FG coordinate, a general function $\mathcal{L}(\bar{\mathcal{L}})$ can be obtained by using Conformal Ward identity, and the result is

$$\mathcal{L}(w_f) = \frac{1}{4} \left(1 - \frac{6h}{c} \frac{\sinh^2 \frac{w_{12}}{2}}{\sinh^2 \frac{w_f - w_1}{2} \sinh^2 \frac{w_f - w_2}{2}} \right) \quad (4.35)$$

which is consistent with (4.14) once the insertion points are substituted. Substituting this function into the integral (4.22) gives the on-shell action in FG coordinate

$$I_{\text{FG}}^{BR} = -\frac{c}{24\pi} \int_{\partial\mathcal{M}} d^2 w_f \sqrt{g^{(0)}} f_{\text{FG}}(w_f, \bar{w}_f) \quad (4.36)$$

where

$$f_{\text{FG}} = 4 (\mathcal{L}\bar{\mathcal{L}})^{\frac{1}{2}} = \left| 1 - \frac{(1 - \alpha^2) \text{csch}^2 \beta}{(\coth \beta - \cosh w_f)^2} \right| \quad (4.37)$$

To verify whether I_{FG}^{BR} yields the inverse of the two-point correlation function, i.e.,

$$\frac{e^{-I_{\text{FG}}^{BR}}}{e^{-I_{\text{global, vacuum}}}} \stackrel{?}{=} \left(\frac{\epsilon^2}{2 \sinh \frac{w_{12}}{2} \times 2 \sinh \frac{\bar{w}_{12}}{2}} \right)^{-2h}, \quad (4.38)$$

we need to know the result of the above integral. However, it is challenging to evaluate this integral analytically and verify the equality, although some numerical evidence and perturbative results suggest that this equality does not hold. In order to provide a more definitive answer, here we take the other way around as follows.

Let us first revisit the on-shell action in FG coordinates. For a generic upper boundary $z_f(w_f, \bar{w}_f)$, the action is given by

$$I_{\text{FG}} = -\frac{c}{12\pi} \int_{\partial\mathcal{M}} d^2 w \sqrt{g^{(0)}} (z_f^{-2} + z_f^2 \mathcal{L}\bar{\mathcal{L}}) \quad (4.39)$$

in which the integrand is a monotonic function of z since the range of z is limited to $0 < z_f^2 < (\mathcal{L}\bar{\mathcal{L}})^{-\frac{1}{2}} = z_w^2, z_f \geq 0$. Now assuming the action I_{FG} exactly gives the inverse

¹¹In global AdS and BTZ spacetimes, we do not impose an identification between the two edges; hence, the boundary geometry is not a torus.

of the two-point function, then it's straightforward to show the upper boundary surface is determined by

$$z_f^2 \mathcal{L}(w_f) \bar{\mathcal{L}}(\bar{w}_f) + z_f^{-2} = \frac{1 + \frac{(1-\alpha^2)}{4} \frac{|\sinh \frac{w_{12}}{2}|^2}{\left| \sinh \frac{w_f-w_1}{2} \sinh \frac{w_f-w_2}{2} \right|^2}}{2}. \quad (4.40)$$

A key observation is

$$\left(\frac{1 + \frac{(1-\alpha^2)}{4} \frac{|\sinh \frac{w_{12}}{2}|^2}{\left| \sinh \frac{w_f-w_1}{2} \sinh \frac{w_f-w_2}{2} \right|^2}}{2} \right)^2 - 4\mathcal{L}(w_f) \bar{\mathcal{L}}(\bar{w}_f) = \frac{1}{4} \left(\frac{\sinh \frac{w_{f,12}}{2}}{\sinh \frac{w_f-w_1}{2} \sinh \frac{w_f-w_2}{2}} + \text{Conjugate} \right)^2 \quad (4.41)$$

which is always non-negative. This observation implies that for a given boundary coordinate, the point $z_f(w_f, \bar{w}_f)$ on this surface is lower than that in the wall

$$z_f^2 \leq z_w^2 = (\mathcal{L} \bar{\mathcal{L}})^{-\frac{1}{2}}. \quad (4.42)$$

The result is the surface, under which the on-shell action yields the inverse of the correlation function, lies entirely outside the wall except at the singularity. Besides, the action between the wall and this surface is nonzero. Supporting evidence arises in the limit $\beta \rightarrow 0$, where the surface $z_f \rightarrow \frac{2}{1+\sqrt{1-\alpha^2}}$ and $z_w \rightarrow \frac{2}{\alpha}$. Clearly the surface z_f is under the wall. In this limit, the on-shell action outside the the surface $z_f(w_f, \bar{w}_f)$ is given by

$$\begin{aligned} I_{\text{FG}, \beta=0} &= -\frac{c}{12\pi} \int_{\partial \mathcal{M}} d^2 w \sqrt{g^{(0)}} \left(\frac{1}{2} + \frac{1-\alpha^2}{2} \right) = I_{\text{global, vacuum}} - \frac{h}{\pi} WT \\ &= I_{\text{global, vacuum}} - 2h \log \frac{\Lambda}{\epsilon}, \quad W = 2\pi \end{aligned} \quad (4.43)$$

which is smaller than $I_{\text{FG}, \beta=0}^{BR} = -\frac{c\alpha^2}{24\pi} WT$. Here, the identification between the Euclidean time direction and the radial direction in the complex plane leads to $T = \log \frac{\Lambda}{\epsilon}$ [21]. Clearly, the inverse of the one-point function can then be read from the partition function

$$\frac{e^{-I_{\text{FG}, \beta=0}}}{e^{-I_{\text{global, vacuum}}}} = \left(\frac{\Lambda}{\epsilon} \right)^\Delta, \quad (4.44)$$

which is consistent with the above discussion. Therefore, I_{FG}^{BR} cannot give the inverse of the two-point function in this case, and

$$I_{\text{FG}}^{BR} > I_{\text{global, vacuum}} - 2h \log \frac{2 \sinh \frac{w_{12}}{2} \times 2 \sinh \frac{\bar{w}_{12}}{2}}{\epsilon^2} \quad (4.45)$$

In conclusion, the partition function in the FG coordinate is exactly smaller than the inverse of the correlation function

$$\frac{e^{-I_{\text{FG}}^{BR}}}{e^{-I_{\text{global, vacuum}}}} < \left(\frac{\epsilon^2}{2 \sinh \frac{w_{12}}{2} \times 2 \sinh \frac{\bar{w}_{12}}{2}} \right)^{-2h}. \quad (4.46)$$

On-shell action of deformed BTZ black hole

In deformed BTZ black hole, the determinant of the metric

$$\sqrt{g} = \frac{1}{z^3} \quad (4.47)$$

is invariant as expected, and the induced metric defined at a naive cutoff $z = \epsilon$ is given by

$$\begin{aligned} \sqrt{h} &= \frac{1}{\epsilon^2} - \frac{1}{2z_H^2} \left(1 + \frac{1 - \alpha^2}{\cosh^2 \beta} \frac{1}{\left| \cosh \frac{w}{z_H} - \tanh \beta \right|^2} \right) \\ &= \frac{1}{\epsilon^2} - \frac{1}{2z_H^2} \left(1 + \frac{1 - \alpha^2}{4} \frac{\left| \sinh \frac{w_{12}}{2z_H} \right|^2}{\left| \sinh \frac{w-w_1}{2z_H} \right|^2 \left| \sinh \frac{w-w_2}{2z_H} \right|^2} \right) \end{aligned} \quad (4.48)$$

where the light-cone coordinate is defined as follows

$$w = x + i\tau, \quad w_{1,2} = \pm iz_H \cos^{-1}(\tanh \beta). \quad (4.49)$$

The on-shell action defined in this constructed solution is

$$\begin{aligned} I^{BR} &= -\frac{1}{16\pi G_N} \int_{\mathcal{M}} \sqrt{g} (R + 2) - \frac{1}{8\pi G_N} \int_{\partial\mathcal{M}} \sqrt{h} (K - 1) + m \int_{\Gamma} \sqrt{\gamma} \\ &= -\frac{WT}{16\pi G_N z_H^2} + \frac{h \left| \sinh \frac{w_{12}}{2z_H} \right|^2}{4\pi z_H^2} \int_{\partial\mathcal{M}} \frac{\sqrt{g^{(0)}} d^2 w}{\left| \sinh \frac{w-w_1}{2z_H} \right|^2 \left| \sinh \frac{w-w_2}{2z_H} \right|^2} \\ &= I_{\text{BTZ, vacuum}} + 2h \log \frac{2z_H \sinh \frac{w_{12}}{2z_H} \times 2z_H \sinh \frac{\bar{w}_{12}}{2z_H}}{\epsilon^2} + I_{\text{bdy}}. \end{aligned} \quad (4.50)$$

Here, W and $T = 2\pi z_H$ represent the width and the length of boundary cylinder of the deformed BTZ black hole, respectively. In the final step, we applied the transformation $u = e^{w/z_H}$ and the result is

$$\int_{\partial\mathcal{M}} \frac{\sqrt{g^{(0)}} dwd\bar{w}}{\left| \sinh \frac{w-w_1}{2z_H} \right|^2 \left| \sinh \frac{w-w_2}{2z_H} \right|^2} = \int_{\partial\mathcal{M}} \frac{16z_H^2 |u_1| |u_2| \sqrt{g^{(0)}} dudv}{|u - u_1|^2 |u - u_2|^2} = \frac{32\pi z_H^2 |u_1| |u_2|}{|u_{12}|^2} \log \frac{|u_{12}|^2}{(2\delta)^2}. \quad (4.51)$$

With

$$\frac{|u_1| |u_2|}{|u_{12}|^2} = \frac{1}{4 \sinh \frac{w_{12}}{2z_H} \sinh \frac{\bar{w}_{12}}{2z_H}}, \quad (4.52)$$

up to an identification

$$\frac{1}{\epsilon^2} = \frac{|u_1| |u_2|}{4z_H^2 \delta^2}, \quad (4.53)$$

we obtain the result presented above. The discussion about the boundary term follows an analogy to that in global AdS. However, due to the specific definition of the light-cone coordinate in this context, the two insertions are mapped to the unit circle with a phase difference of π . If the spatial direction is non-compact, then the boundary term I_{bdy} vanishes. Otherwise, the boundary term contributes at a constant order as follows

$$I_{bdy} = 2h \log \frac{\cosh W - 1}{\cosh W + 1 - 2 \tanh^2 \beta}. \quad (4.54)$$

where the range of x is set to $-\frac{W}{2} < x < \frac{W}{2}$. So the leading order partition function gives

$$\frac{e^{-I_{BR}}}{e^{-I_{BTZ, \text{vacuum}}}} \approx \left(\frac{\epsilon^2}{2z_H \sinh \frac{w_{12}}{2z_H} \times 2z_H \sinh \frac{\bar{w}_{12}}{2z_H}} \right)^\Delta, \quad (4.55)$$

which is exactly the two-point function in BTZ blackhole.

In the FG coordinate of the deformed BTZ black hole, substituting the $\mathcal{L}(\bar{\mathcal{L}})$ function (4.15) into the expression (4.21) of the wall and the integral (4.22) yields the location of the wall and the on-shell action I_{FG}^{BR} , respectively, in this case. As previously discussed, it is challenging to directly verify whether I_{FG}^{BR} gives the inverse of the two-point function

$$\frac{e^{-I_{FG}^{BR}}}{e^{-I_{BTZ, \text{vacuum}}}} \stackrel{?}{=} \left(\frac{\epsilon^2}{2z_H \sinh \frac{w_{12}}{2} \times 2z_H \sinh \frac{\bar{w}_{12}}{2}} \right)^{-2h}. \quad (4.56)$$

Therefore, here we take the other way around as in previous case. The surface, under which the on-shell action in FG coordinates yields the inverse of the correlation function, is determined by

$$z_f^2 \mathcal{L}(w_f) \bar{\mathcal{L}}(\bar{w}_f) + z_f^{-2} = \frac{1}{2z_H^2} \left(1 + \frac{1 - \alpha^2}{4} \frac{\left| \sinh \frac{w_{12}}{2z_H} \right|^2}{\left| \sinh \frac{w-w_1}{2z_H} \right|^2 \left| \sinh \frac{w-w_2}{2z_H} \right|^2} \right). \quad (4.57)$$

Notice that

$$\frac{\left(1 + \frac{1 - \alpha^2}{4} \frac{\left| \sinh \frac{w_{f,12}}{2z_H} \right|^2}{\left| \sinh \frac{w_f - w_1}{2z_H} \right|^2 \left| \sinh \frac{w_f - w_2}{2z_H} \right|^2} \right)^2}{4z_H^4} - 4\mathcal{L}\bar{\mathcal{L}} = -\frac{1 - \alpha^2}{4} \left(\frac{\sinh \frac{w_{f,12}}{2z_H}}{\sinh \frac{w_f - w_1}{2z_H} \sinh \frac{w_f - w_2}{2z_H}} - \text{Conjugate} \right)^2 \quad (4.58)$$

which is strictly non-negative. As in global AdS, the result implies that the surface, under which the on-shell action reproduces the inverse of the two-point function, lies entirely outside the wall, except at the singularity. When $\beta \rightarrow 0$, this surface reduces to

$$z_f^{-2} + \mathcal{L}\bar{\mathcal{L}}z_f^2 = \frac{1}{2z_H^2} + \frac{1 - \alpha^2}{2z_H^2} \frac{1}{\cosh \frac{w_f}{z_H} \cosh \frac{\bar{w}_f}{z_H}}. \quad (4.59)$$

In this limit, the on-shell action evaluated under this surface is given by

$$\begin{aligned}
I_{\text{FG},\beta=0} &= -\frac{c}{12\pi} \int_{\partial\mathcal{M}} d^2w \sqrt{g^{(0)}} \left(\frac{1}{2z_H^2} + \frac{1-\alpha^2}{2z_H^2} \frac{1}{\cosh \frac{w}{z_H} \cosh \frac{\bar{w}}{z_H}} \right) \\
&= -I_{\text{BTZ,vacuum}} - 2h \log \frac{2 \sinh \frac{w_{12}}{2z_H} \times 2 \sinh \frac{\bar{w}_{12}}{2z_H}}{\epsilon^2}
\end{aligned} \tag{4.60}$$

where the boundary insertions reduce to $w_{1,2} = i\tau_{1,2} = \pm i \frac{\pi z_H}{2}$ in this case. Therefore, the partition function $e^{-I_{\text{FG},\beta=0}}$ in the FG gauge gives the inverse of the two-point function.

In conclusion, the on-shell action I_{FG}^{BR} defined in the FG patch does not yield the inverse of the two-point function in this case. Moreover, the former is generally larger than the latter, as demonstrated below

$$I_{\text{FG}}^{BR} > I_{\text{BTZ,vacuum}} - 2h \log \frac{2z_H \sinh \frac{w_{12}}{2z_H} \times 2z_H \sinh \frac{\bar{w}_{12}}{2z_H}}{\epsilon^2}, \tag{4.61}$$

which strengthen our belief that the action inside the FG patch is not always meaningful [21]. We leave this interesting question to the future.

5 Discussion

In this work, we proposed and examined a novel holographic approach for computing the correlation functions of operators in CFTs, refining and generalizing the proposal presented in [27]. We demonstrated that correlation functions can be computed through the on-shell actions of excised geometries in the probe limit by doing numeric and perturbative calculations. These geometries are constructed from various AdS solutions, including Poincaré AdS, global AdS, and BTZ solutions, by excising a wedge bounded by two intersecting EOW branes and the AdS asymptotic boundary. From the perspective of the AdS/BCFT correspondence, this wedge is dual to a BCFT defined in a region with boundary cusps¹².

Additionally, we constructed the backreacted geometries corresponding to the correlation functions using a more direct approach. This involved performing coordinate transformations on the conical geometry. We computed the on-shell actions for these backreacted solutions, as well as for their FG gauges. We found that the on-shell actions of the backreacted solutions are proper to reproduce the correlation functions with no need of taking the probe limit, while they differ from the on-shell actions of the same backreacted geometry in FG gauge. This discrepancy, previously noted in [21], is supported by additional examples in this work. The AdS₃ solutions in the FG gauges, known as the Bañados solutions, are widely utilized in AdS₃ holography. Our findings may reveal deeper insights that have been previously overlooked. A potential approach to addressing this issue involves employing a generalized FG gauge, as proposed in [59]. We discuss several future directions below.

¹²Interestingly, it is recently pointed out in [58] that the BCFT defined within a wedge region with non-smooth corners may exhibit certain singularities in the energy-stress tensor.

Local Quench. As mentioned in Section 4, the backreacted (deformed) solutions can serve as models for studying local quenches. It would be intriguing to investigate other properties, such as entanglement or entwinement [60], within these excised geometries.

Correlation Functions of Boundary Condition Changing (BCC) Operators. In this work, we focused on correlation functions in a CFT. However, when motivating our wedge proposal, we also noted that the generalized AdS/BCFT correspondence allows us to study BCC operators. We proposed a straightforward, albeit perhaps naive, setup for computing the two-point functions of BCC operators. Further exploration in this area would be valuable.

Spinning Operators. Our study concentrated on the correlation functions of scalar operators. Recent work has highlighted interesting developments regarding spinning particles in AdS₃ [61–68]. In particular, the authors of [40] proposed an excised geometry to describe spinning defects. We anticipate that our wedge proposal can also be extended to include correlation functions of spinning operators.

Three-Dimensional C-Metric. Recently, C-metric solutions in AdS₃, which describe accelerating particles or black holes, have garnered renewed attention. As shown in [69,70], a 3D C-metric can be derived from a direct truncation of solutions in four dimensions, which have been explored extensively [71–82]. Recent studies have clarified the holography of the C-metric in three dimensions [83–87]. As pointed out in [86,87], due to the EOW brane construction, the 3D C-metric is naturally dual to a CFT with defects. Therefore, we expect that a suitable excised geometry based on the 3D C-metric will be dual to correlation functions in a CFT with defects or boundaries.

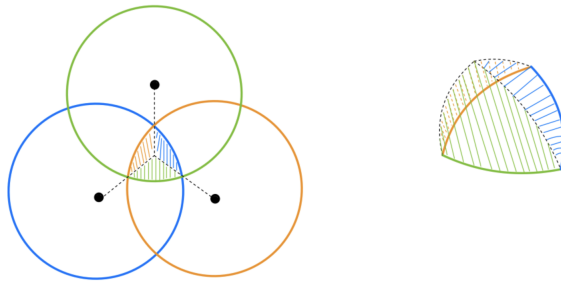


Figure 11: A naive attempt at constructing a wedge for a three-point function, represented as the overlap of three hemispheres.

Higher Dimensions and Higher-Point Functions. Lastly, it would be intriguing to generalize the wedge proposal to higher dimensions, where constructing a wedge geometry is significantly more straightforward than a backreacted geometry. The extension to higher-point functions is essential yet challenging. We have verified that a naive configuration, such as the one illustrated in Figure 11, does not yield valid results. One possible direction is to consider certain holographic polygons [58]. We will leave these explorations for future studies.

Acknowledgments

We thank Bo-Hao Liu and Wen-Bin Pan for the valuable discussion on related topics. We thank Farzad Omidi for discussion and collaboration on related works. T.L would like to especially thank HH for his assistance in completing the figures in this paper. JT is supported by the National Youth Fund No.12105289 and funds from the University of Chinese Academy of Sciences (UCAS), the Kavli Institute for Theoretical Sciences (KITS). T.L and YWS are supported by Project 12035016 of the National Natural Science Foundation of China.

A Wedge in Poincaré AdS₃

In Poincaré AdS₃, the action inside the wedge region is given by¹³

$$\begin{aligned}
I_{\text{AdS,EH}} &= -\frac{1}{16\pi G_N} \int_{\mathcal{M}} \sqrt{g} (R + 2) - \frac{1}{8\pi G_N} \int_{\partial\mathcal{M}} \sqrt{h} (K - 1) \\
&= \frac{1}{8\pi G_N} \int_{-\eta}^{+\eta} d\theta \int_{a^2/\cos^2(\theta)}^{\sqrt{b^2-\epsilon^2}} \frac{d\rho^2}{\rho^2 - b^2} \\
&= \frac{1}{8\pi G_N} \int_{-\eta}^{\eta} \left(2 \log \frac{\epsilon}{b} - \log [1 - \cos^2(\eta) \sec^2(\theta)] \right) d\theta \tag{A.1}
\end{aligned}$$

where the following polar coordinate

$$x_0 = \coth \beta + \rho \sin \theta, \quad x_1 = -\frac{1}{\sinh \beta \tan \eta} + \rho \cos \theta \tag{A.2}$$

and the convention

$$b = \frac{1}{\sin(\eta) \sinh \beta}, \quad a = \frac{1}{\tan(\eta) \sinh \beta} = b \cos(\eta) \tag{A.3}$$

have been adopted. Given the following integral identity

$$\int \log(1 - \cos^2(\eta) \sec^2(\theta)) d\theta = \frac{i}{2} [\text{Li}_2(e^{2i(\theta-\eta)}) + \text{Li}_2(e^{2i(\theta+\eta)}) - 2\text{Li}_2(-e^{2i\theta})] \tag{A.4}$$

and the property of dilogarithm function $\text{Li}_2(z)$

$$\text{Li}_2(z) + \text{Li}_2(-z) = \frac{1}{2} \text{Li}_2(z^2), \tag{A.5}$$

it's straightforward show the result is

$$I_{\text{AdS,EH}} = \frac{1}{8\pi G_N} \left[4\eta \log \frac{\epsilon}{b} - i (\text{Li}_2(e^{2i\eta}) - \text{Li}_2(e^{-2i\eta})) \right]. \tag{A.6}$$

¹³The detail of this calculation can be found in [27], we repeat it here for sake of completeness.

Note that the two edges should be identified once the wedge region is excised. Therefore, when computing the Hayward terms, an overall angle of π should be subtracted. A useful convention is dividing it into two identical pieces, as illustrated below. Given that

$$n_1 \cdot n_0 = -\frac{\epsilon}{b}, \quad \sqrt{\gamma} = \frac{1}{b\epsilon} \quad (\text{A.7})$$

the contribution of the corner term is given by

$$I_{Q_{1,2} \cap \partial\mathcal{M}} = -\frac{2 \times 1}{8\pi G_N} \int_{-\eta}^{\eta} d\theta \sqrt{\gamma} \left(\arccos(n_1 \cdot n_0) - \frac{\pi}{2} \right) = -\frac{\eta}{2\pi G_N}. \quad (\text{A.8})$$

which is of constant order. Although we include this term here for completeness, the contribution of this term will be skipped, as we are primarily concerned with the leading-order logarithmic divergence arising from the Weyl anomaly of the dual BCFT. When the deficit angle η is small, the leading on-shell action is given by

$$\begin{aligned} I_{gravity,W} &= I_{\text{AdS,EH}} + I_{Q_{1,2} \cap \partial\mathcal{M}} \\ &= \frac{1}{8\pi G_N} \left[4\eta \log \frac{\epsilon}{b} - i \left(\text{Li}_2(e^{2i\eta}) - \text{Li}_2(e^{-2i\eta}) \right) - 4\eta \right] \\ &\approx \frac{\eta}{4\pi G_N} \log \frac{\epsilon^2}{4 \text{csch}^2 \beta} + \mathcal{O}(\eta^3). \end{aligned} \quad (\text{A.9})$$

B The detail of the integral

In this appendix we will show the detail of the following integral

$$I_{\text{Euc}} = \int_{\partial\mathcal{M}} \frac{\sqrt{g^{(0)}} d^2 z}{|z - z_1|^2 |z - z_2|^2}, \quad (\text{B.1})$$

which is defined on the whole complex plane with the metric

$$ds_{bdy}^2 = g_{ij}^{(0)} dx^i dx^j = dz d\bar{z}. \quad (\text{B.2})$$

This integral can also be evaluated using the Feynman parameter technique [88], with further details about this integral provided in [89]. Without loss of generality, we assume

$$|z_2| \geq |z_1|, \quad (\text{B.3})$$

and introduce the following polar coordinate

$$z = \rho e^{i\theta}, \quad \bar{z} = \rho e^{-i\theta}. \quad (\text{B.4})$$

Using polar coordinates, the integral can be evaluated by first completing the integration over θ . The resulting primitive function is given by

$$\begin{aligned}
f(\rho, \theta) &= f_1(\theta, \rho) + f_2(\theta, \rho) + f_3(\theta, \rho) \tag{B.5} \\
f_1(\theta, \rho) &= \frac{\theta (|z_1|^2 |z_2|^2 - \rho^4)}{(|z_1|^2 - \rho^2) (\bar{z}_1 z_2 - \rho^2) (z_1 \bar{z}_2 - \rho^2) (|z_2|^2 - \rho^2)} \\
f_2(\theta, \rho) &= \frac{i}{|z_1|^2 - \rho^2} \left[\frac{\bar{z}_1}{\bar{z}_{12} (\bar{z}_1 z_2 - \rho^2)} \log(\bar{z}_1 - \rho e^{-i\theta}) - \frac{z_1}{z_{12} (z_1 \bar{z}_2 - \rho^2)} \log(z_1 - \rho e^{i\theta}) \right] \\
f_3(\theta, \rho) &= \frac{i}{|z_2|^2 - \rho^2} \left[-\frac{\bar{z}_2}{\bar{z}_{12} (z_1 \bar{z}_2 - \rho^2)} \log(\bar{z}_2 - \rho e^{-i\theta}) + \frac{z_2}{z_{12} (\bar{z}_1 z_2 - \rho^2)} \log(z_2 - \rho e^{i\theta}) \right].
\end{aligned}$$

By applying the residue theorem, it's straightforward to show the following: when $0 < \rho < |z_{1,2}|$, the second and third term vanish; when $\rho > |z_{1,2}|$, the logarithm function in above contributes $\pm 2\pi i$, as illustrated in the Figure 12. the contribution of the integral consists of three parts, depending on whether the radius ρ lies within the specified interval $(0, |z_1|)$, $(|z_1|, |z_2|)$ or $(|z_2|, \infty)$. The precise result is given by

$$\begin{aligned}
\mathbf{I}_{\text{Euc}} &= \mathbf{I}_{\text{Euc}}^1 + \mathbf{I}_{\text{Euc}}^2 + \mathbf{I}_{\text{Euc}}^3 \tag{B.6} \\
\mathbf{I}_{\text{Euc}}^1 &= \pi \int_0^{(|z_1|-\delta)^2} \frac{(|z_1|^2 |z_2|^2 - \rho^4) d\rho^2}{(|z_1|^2 - \rho^2) (\bar{z}_1 z_2 - \rho^2) (z_1 \bar{z}_2 - \rho^2) (|z_2|^2 - \rho^2)} \\
\mathbf{I}_{\text{Euc}}^2 &= \pi \int_{(|z_1|+\delta)^2}^{(|z_2|-\delta)^2} \frac{(|z_2|^2 - |z_1|^2) d\rho^2}{|z_{12}|^2 (\rho^2 - |z_1|^2) (|z_2|^2 - \rho^2)} \\
\mathbf{I}_{\text{Euc}}^3 &= \pi \int_{(|z_2|+\delta)^2}^{\infty} \frac{(\rho^4 - |z_1|^2 |z_2|^2) d\rho^2}{(\rho^2 - |z_1|^2) (\rho^2 - \bar{z}_1 z_2) (\rho^2 - z_1 \bar{z}_2) (\rho^2 - |z_2|^2)}
\end{aligned}$$

where the radial regulator δ is introduced. Performing the integral over ρ and combining all these three terms give the leading result

$$\mathbf{I}_{\text{Euc}} = \frac{2\pi}{|z_{12}|^2} \log \frac{|z_{12}|^2}{(2\delta)^2}. \tag{B.7}$$

Up to a rescale of the regulator $\epsilon = 2\delta$, the result of this integral is

$$\mathbf{I}_{\text{Euc}} = \frac{2\pi}{|z_{12}|^2} \log \frac{|z_{12}|^2}{\epsilon^2}. \tag{B.8}$$

When we evaluated the above integral, we have implicitly assumed that the integration is carried out over the entire complex plane. However, if the integration region is restricted to a annulus, $\rho_a \leq \rho \leq \rho_b$, the following boundary term should be included:

$$\frac{\pi}{|z_{12}|^2} \left[\log \frac{(|z_1|^2 - \rho_a^2) (|z_2|^2 - \rho_a^2)}{(\bar{z}_1 z_2 - \rho_a^2) (z_1 \bar{z}_2 - \rho_a^2)} + \log \frac{(\rho_b^2 - |z_1|^2) (\rho_b^2 - |z_2|^2)}{(\rho_b^2 - \bar{z}_1 z_2) (\rho_b^2 - z_1 \bar{z}_2)} \right] \tag{B.9}$$

which is of constant order. When $\rho_a \ll |z_{1,2}| \ll \rho_b$, this boundary term can be neglected.

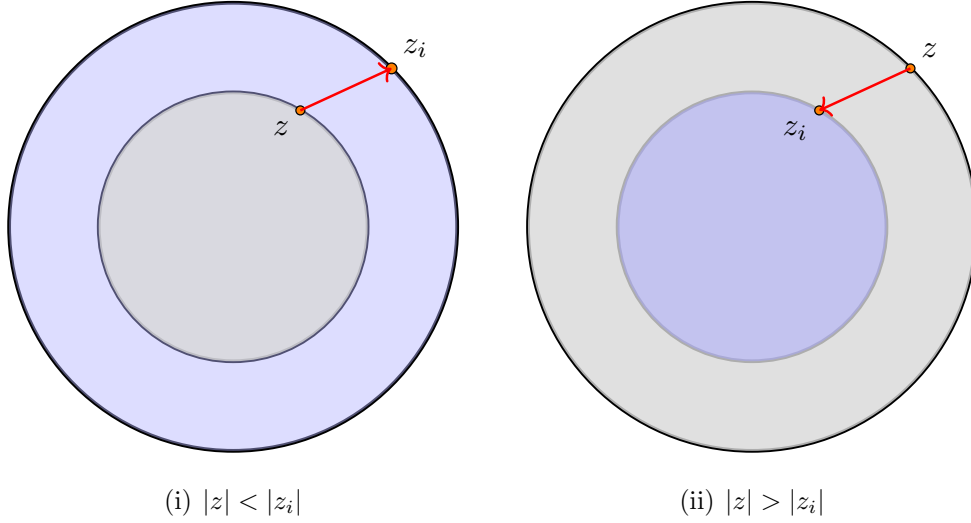


Figure 12: Two cases of the integral

C Higher-order corrections

In this appendix, we include the higher-order corrections to the on-shell action of both the global wedge and the BTZ wedge. Since the integrand is quite complicated, we will only present the result and compare it with the numerical result.

Global

In global AdS, we first recall the leading-order result for convenience,

$$-8\pi G_N I_{gravity,W} = -2\eta \log \frac{\epsilon^2}{4 \sin \frac{w_{12}}{2} \sin \frac{\bar{w}_{12}}{2}} - 2\eta \left(1 + \cosh \beta \log \left(\coth \frac{\beta}{2} \right) \right). \quad (\text{C.1})$$

The sub-leading correction is

$$\frac{\eta^3}{9} \left[5 - 3 \cosh(2\beta) - 6 \cosh(\beta) \sinh^2(\beta) \log \left(\tanh \frac{\beta}{2} \right) \right], \quad (\text{C.2})$$

and the second and third-order corrections are given by

$$\frac{\eta^5 \left[23 - 60 \cosh(2\beta) + 45 \cosh(4\beta) + 30 \sinh^2(\beta) (\cosh \beta + 3 \cosh(3\beta)) \log \left(\tanh \frac{\beta}{2} \right) \right]}{900}, \quad (\text{C.3})$$

$$\frac{\eta^7 \left[32 - 21 (6 + 90 \cosh(4\beta) + (2 \cosh \beta - 15 \cosh(3\beta) + 45 \cosh(5\beta)) \log \left(\tanh \frac{\beta}{2} \right)) \sinh^2 \beta \right]}{52920}. \quad (\text{C.4})$$

As shown in the Table 1, once the higher-order corrections are included, the deviation approaches zero.

Set up	Leading	Sub-leading	Second	Third	Numerical
$\beta = 0.01, \eta = 1.57$	100.257160	101.118245	101.202616	101.216902	101.220328
$\beta = 2, \eta = 1.57$	76.666174	78.361057	78.521957	78.547600	78.553275
$\beta = 5, \eta = 1.57$	57.787430	59.507320	59.676879	59.703443	59.712172

Table 1: Comparison between numerical and perturbative result when $\epsilon = 10^{-6}$.

Set up	Leading	Sub-leading	Second	Third	Numerical
$\beta = 0.01, \eta = 1.404717$	78.668659	81.103846	81.859245	82.259073	83.090989
$\beta = 0.1, \eta = 1.323866$	73.765806	75.613561	76.050023	76.230839	76.414456
$\beta = 0.5, \eta = 0.981374$	53.404152	53.960138	54.001459	54.007191	54.008366
$\beta = 1, \eta = 0.634524$	33.402881	33.529183	33.531837	33.531939	33.531944

Table 2: Comparison between numerical and perturbative result in BTZ black hole when $\mathcal{G} < 1$ and the parameters are set as $\epsilon = 10^{-6}$, $z_H = 1$.

BTZ

In the BTZ black hole, when $\mathcal{G} < 1$, the perturbation result at leading order is given by

$$-8\pi G_N I_{gravity,W} = -2\eta \left(\log \frac{\epsilon^2}{4z_H^2 \operatorname{sech}^2 \beta} + 1 + \cos^{-1}(\tanh \beta) \sinh \beta \right). \quad (\text{C.5})$$

The sub-leading correction is given by

$$\frac{\eta^3 (3 \cosh(2\beta) - 6 \sinh(\beta) \cosh^2(\beta) \cos^{-1}(\tanh(\beta)) + 5)}{9}, \quad (\text{C.6})$$

and the second and third-order corrections are

$$\frac{\eta^5 (60 \cosh(2\beta) + 45 \cosh(4\beta) + 30(\sinh(\beta) - 3 \sinh(3\beta)) \cosh^2(\beta) \cos^{-1}(\tanh(\beta)) + 23)}{900}, \quad (\text{C.7})$$

$$\frac{\eta^7 (1071 \cosh(2\beta) + 1890 \cosh(4\beta) + 945 \cosh(6\beta) + 190)}{105840} - \frac{\eta^7 (2 \sinh(\beta) + 15(\sinh(3\beta) + 3 \sinh(5\beta))) \cosh^2(\beta) \cos^{-1}(\tanh \beta)}{2520} \quad (\text{C.8})$$

As illustrated in Table 2, for a fixed value of \mathcal{G} , as the boost parameter β increases and the range of deficit angle η decreases, the deviation between the numerical and perturbation results becomes negligible.

References

- [1] J. M. Maldacena, “The Large N limit of superconformal field theories and supergravity,” *Adv. Theor. Math. Phys.* **2** (1998) 231–252, [arXiv:hep-th/9711200](#).
- [2] O. Aharony, S. S. Gubser, J. M. Maldacena, H. Ooguri, and Y. Oz, “Large N field theories, string theory and gravity,” *Phys. Rept.* **323** (2000) 183–386, [arXiv:hep-th/9905111](#).
- [3] E. Witten, “Anti-de Sitter space and holography,” *Adv. Theor. Math. Phys.* **2** (1998) 253–291, [arXiv:hep-th/9802150](#).
- [4] A. Strominger and C. Vafa, “Microscopic origin of the Bekenstein-Hawking entropy,” *Phys. Lett. B* **379** (1996) 99–104, [arXiv:hep-th/9601029](#).
- [5] I. R. Klebanov and E. Witten, “AdS / CFT correspondence and symmetry breaking,” *Nucl. Phys. B* **556** (1999) 89–114, [arXiv:hep-th/9905104](#).
- [6] L. Susskind and E. Witten, “The Holographic bound in anti-de Sitter space,” [arXiv:hep-th/9805114](#).
- [7] T. Banks, M. R. Douglas, G. T. Horowitz, and E. J. Martinec, “AdS dynamics from conformal field theory,” [arXiv:hep-th/9808016](#).
- [8] G. T. Horowitz and N. Itzhaki, “Black holes, shock waves, and causality in the AdS / CFT correspondence,” *JHEP* **02** (1999) 010, [arXiv:hep-th/9901012](#).
- [9] S. S. Gubser, I. R. Klebanov, and A. M. Polyakov, “Gauge theory correlators from noncritical string theory,” *Phys. Lett. B* **428** (1998) 105–114, [arXiv:hep-th/9802109](#).
- [10] D. Z. Freedman, S. D. Mathur, A. Matusis, and L. Rastelli, “Correlation functions in the CFT(d) / AdS(d+1) correspondence,” *Nucl. Phys. B* **546** (1999) 96–118, [arXiv:hep-th/9804058](#).
- [11] V. Balasubramanian and S. F. Ross, “Holographic particle detection,” *Phys. Rev. D* **61** (2000) 044007, [arXiv:hep-th/9906226](#).
- [12] V. Balasubramanian, A. Bernamonti, B. Craps, V. Keränen, E. Keski-Vakkuri, B. Müller, L. Thorlacius, and J. Vanhoof, “Thermalization of the spectral function in strongly coupled two dimensional conformal field theories,” *JHEP* **04** (2013) 069, [arXiv:1212.6066 \[hep-th\]](#).
- [13] J. Kastikainen and S. Shashi, “Structure of holographic BCFT correlators from geodesics,” *Phys. Rev. D* **105** no. 4, (2022) 046007, [arXiv:2109.00079 \[hep-th\]](#).

- [14] C.-M. Chang and Y.-H. Lin, “Bootstrap, universality and horizons,” *JHEP* **10** (2016) 068, [arXiv:1604.01774 \[hep-th\]](#).
- [15] B. Chen, J.-q. Wu, and J.-j. Zhang, “Holographic Description of 2D Conformal Block in Semi-classical Limit,” *JHEP* **10** (2016) 110, [arXiv:1609.00801 \[hep-th\]](#).
- [16] K. B. Alkalaev and V. A. Belavin, “Holographic duals of large- c torus conformal blocks,” *JHEP* **10** (2017) 140, [arXiv:1707.09311 \[hep-th\]](#).
- [17] E. Hijano, P. Kraus, E. Perlmutter, and R. Snively, “Semiclassical Virasoro blocks from AdS₃ gravity,” *JHEP* **12** (2015) 077, [arXiv:1508.04987 \[hep-th\]](#).
- [18] E. Hijano, P. Kraus, E. Perlmutter, and R. Snively, “Witten Diagrams Revisited: The AdS Geometry of Conformal Blocks,” *JHEP* **01** (2016) 146, [arXiv:1508.00501 \[hep-th\]](#).
- [19] J. Abajian, F. Aprile, R. C. Myers, and P. Vieira, “Holography and correlation functions of huge operators: spacetime bananas,” *JHEP* **12** (2023) 058, [arXiv:2306.15105 \[hep-th\]](#).
- [20] J. Abajian, F. Aprile, R. C. Myers, and P. Vieira, “Correlation functions of huge operators in AdS₃/CFT₂: domes, doors and book pages,” *JHEP* **03** (2024) 118, [arXiv:2307.13188 \[hep-th\]](#).
- [21] J. Tian, T. Lai, and F. Omid, “Spacetime Bananas with EOW Branes and Spins,” [arXiv:2410.18729 \[hep-th\]](#).
- [22] K. Krasnov, “Holography and Riemann surfaces,” *Adv. Theor. Math. Phys.* **4** (2000) 929–979, [arXiv:hep-th/0005106](#).
- [23] L. Hadasz, Z. Jaskolski, and M. Piatek, “Classical geometry from the quantum Liouville theory,” *Nucl. Phys. B* **724** (2005) 529–554, [arXiv:hep-th/0504204](#).
- [24] D. Harlow, J. Maltz, and E. Witten, “Analytic Continuation of Liouville Theory,” *JHEP* **12** (2011) 071, [arXiv:1108.4417 \[hep-th\]](#).
- [25] H.-J. Matschull, “Black hole creation in (2+1)-dimensions,” *Class. Quant. Grav.* **16** (1999) 1069–1095, [arXiv:gr-qc/9809087](#).
- [26] J. Louko, D. Marolf, and S. F. Ross, “On geodesic propagators and black hole holography,” *Phys. Rev. D* **62** (2000) 044041, [arXiv:hep-th/0002111](#).
- [27] P. Caputa and D. Ge, “Entanglement and geometry from subalgebras of the Virasoro algebra,” *JHEP* **06** (2023) 159, [arXiv:2211.03630 \[hep-th\]](#).
- [28] M. Nozaki, T. Numasawa, and T. Takayanagi, “Holographic Local Quenches and Entanglement Density,” *JHEP* **05** (2013) 080, [arXiv:1302.5703 \[hep-th\]](#).

- [29] C. R. Graham, “Charles fefferman,” *Astérisque* **131** (1985) 95–116.
- [30] C. Fefferman and C. R. Graham, “The ambient metric,” *Ann. Math. Stud.* **178** (2011) 1–128, [arXiv:0710.0919 \[math.DG\]](#).
- [31] T. Takayanagi, “Holographic Dual of BCFT,” *Phys. Rev. Lett.* **107** (2011) 101602, [arXiv:1105.5165 \[hep-th\]](#).
- [32] M. Fujita, T. Takayanagi, and E. Tonni, “Aspects of AdS/BCFT,” *JHEP* **11** (2011) 043, [arXiv:1108.5152 \[hep-th\]](#).
- [33] P. Caputa, J. Simón, A. Štikonas, and T. Takayanagi, “Quantum Entanglement of Localized Excited States at Finite Temperature,” *JHEP* **01** (2015) 102, [arXiv:1410.2287 \[hep-th\]](#).
- [34] D. V. Fursaev and S. N. Solodukhin, “On the description of the Riemannian geometry in the presence of conical defects,” *Phys. Rev. D* **52** (1995) 2133–2143, [arXiv:hep-th/9501127](#).
- [35] J. D. Brown and M. Henneaux, “Central Charges in the Canonical Realization of Asymptotic Symmetries: An Example from Three-Dimensional Gravity,” *Commun. Math. Phys.* **104** (1986) 207–226.
- [36] G. Hayward, “Gravitational action for space-times with nonsmooth boundaries,” *Phys. Rev. D* **47** (1993) 3275–3280.
- [37] J. Boruch, P. Caputa, D. Ge, and T. Takayanagi, “Holographic path-integral optimization,” *JHEP* **07** (2021) 016, [arXiv:2104.00010 \[hep-th\]](#). [Erratum: *JHEP* **09**, 111 (2022)].
- [38] J. Chandra, S. Collier, T. Hartman, and A. Maloney, “Semiclassical 3D gravity as an average of large- c CFTs,” *JHEP* **12** (2022) 069, [arXiv:2203.06511 \[hep-th\]](#).
- [39] H. Geng, S. Lüster, R. K. Mishra, and D. Wakeham, “Holographic BCFTs and Communicating Black Holes,” *jhep* **08** (2021) 003, [arXiv:2104.07039 \[hep-th\]](#).
- [40] Y. Kusuki and Z. Wei, “AdS/BCFT from conformal bootstrap: construction of gravity with branes and particles,” *JHEP* **01** (2023) 108, [arXiv:2210.03107 \[hep-th\]](#).
- [41] M. Miyaji and C. Murdia, “Holographic BCFT with a Defect on the End-of-the-World brane,” *JHEP* **11** (2022) 123, [arXiv:2208.13783 \[hep-th\]](#).
- [42] S. Biswas, J. Kastikainen, S. Shashi, and J. Sully, “Holographic BCFT spectra from brane mergers,” *JHEP* **11** (2022) 158, [arXiv:2209.11227 \[hep-th\]](#).

- [43] J. Tian and X. Xu, “Negative Rényi entropy and brane intersection,” *JHEP* **04** (2023) 142, [arXiv:2302.13489 \[hep-th\]](#).
- [44] J. L. Cardy, “Boundary conditions, fusion rules and the verlinde formula,” *Nuclear Physics B* **324** no. 3, (1989) 581–596.
- [45] J. L. Cardy, “Boundary conformal field theory,” [arXiv:hep-th/0411189](#).
- [46] A. Almheiri and H. W. Lin, “The entanglement wedge of unknown couplings,” *JHEP* **08** (2022) 062, [arXiv:2111.06298 \[hep-th\]](#).
- [47] I. Affleck and A. W. Ludwig, “The fermi edge singularity and boundary condition changing operators,” *Journal of Physics A: Mathematical and General* **27** no. 16, (1994) 5375.
- [48] M. Henningson and K. Skenderis, “The holographic weyl anomaly,” *Journal of High Energy Physics* **1998** no. 07, (1998) 023.
- [49] P. C. Aichelburg and R. U. Sexl, “On the gravitational field of a massless particle,” *General Relativity and Gravitation* **2** no. 4, (1971) 303–312.
- [50] T. Dray and G. ’t Hooft, “The effect of spherical shells of matter on the schwarzschild black hole,” *Communications in Mathematical Physics* **99** no. 4, (1985) 613–625.
- [51] T. Dray and G. Hooft, “The gravitational shock wave of a massless particle,” *Nuclear physics B* **253** (1985) 173–188.
- [52] M. Hotta and M. Tanaka, “Shock-wave geometry with nonvanishing cosmological constant,” *Classical and Quantum Gravity* **10** no. 2, (1993) 307.
- [53] K. Sfetsos, “On gravitational shock waves in curved space-times,” *Nucl. Phys. B* **436** (1995) 721–745, [arXiv:hep-th/9408169](#).
- [54] M. Banados, M. Henneaux, C. Teitelboim, and J. Zanelli, “Geometry of the (2+1) black hole,” *Phys. Rev. D* **48** (1993) 1506–1525, [arXiv:gr-qc/9302012](#). [Erratum: *Phys.Rev.D* **88**, 069902 (2013)].
- [55] M. Banados, C. Teitelboim, and J. Zanelli, “The Black hole in three-dimensional space-time,” *Phys. Rev. Lett.* **69** (1992) 1849–1851, [arXiv:hep-th/9204099](#).
- [56] A. Štikonas, “Scrambling time from local perturbations of the rotating BTZ black hole,” *JHEP* **02** (2019) 054, [arXiv:1810.06110 \[hep-th\]](#).
- [57] M. Banados, “Three-dimensional quantum geometry and black holes,” *AIP Conf. Proc.* **484** no. 1, (1999) 147–169, [arXiv:hep-th/9901148](#).

- [58] R.-X. Miao, “Casimir effect and holographic dual of wedges,” *JHEP* **06** (2024) 084, [arXiv:2404.11783 \[hep-th\]](#).
- [59] G. Arenas-Henriquez, F. Diaz, and D. Rivera-Betancour, “Generalized Fefferman-Graham gauge and boundary Weyl structures,” [arXiv:2411.12513 \[hep-th\]](#).
- [60] V. Balasubramanian, B. D. Chowdhury, B. Czech, and J. de Boer, “Entwinement and the emergence of spacetime,” *JHEP* **01** (2015) 048, [arXiv:1406.5859 \[hep-th\]](#).
- [61] M. Mathisson, *Neue mechanik materieller systeme*. 1937.
- [62] A. Papapetrou, “Spinning test-particles in general relativity. i,” *Proceedings of the Royal Society of London. Series A. Mathematical and Physical Sciences* **209** no. 1097, (1951) 248–258.
- [63] W. G. Dixon, “Dynamics of extended bodies in general relativity. i. momentum and angular momentum,” *Proceedings of the Royal Society of London. A. Mathematical and Physical Sciences* **314** no. 1519, (1970) 499–527.
- [64] A. Castro, S. Detournay, N. Iqbal, and E. Perlmutter, “Holographic entanglement entropy and gravitational anomalies,” *JHEP* **07** (2014) 114, [arXiv:1405.2792 \[hep-th\]](#).
- [65] C.-M. Chang, D. M. Ramirez, and M. Rangamani, “Spinning constraints on chaotic large c CFTs,” *JHEP* **03** (2019) 068, [arXiv:1812.05585 \[hep-th\]](#).
- [66] Z. Li, “Spinning particle geometries in $\text{AdS}_3/\text{CFT}_2$,” *JHEP* **05** (2024) 216, [arXiv:2403.05524 \[hep-th\]](#).
- [67] O. Baake and J. Zanelli, “Quantum backreaction for overspinning BTZ geometries,” *Phys. Rev. D* **107** no. 8, (2023) 084015, [arXiv:2301.04256 \[hep-th\]](#).
- [68] M. Briceño, C. Martínez, and J. Zanelli, “Overspinning naked singularities in AdS_3 spacetime,” *Phys. Rev. D* **104** no. 4, (2021) 044023, [arXiv:2105.06488 \[gr-qc\]](#).
- [69] M. Astorino, “Accelerating black hole in 2+1 dimensions and 3+1 black (st)ring,” *JHEP* **01** (2011) 114, [arXiv:1101.2616 \[gr-qc\]](#).
- [70] W. Xu, K. Meng, and L. Zhao, “Accelerating BTZ spacetime,” *Class. Quant. Grav.* **29** (2012) 155005, [arXiv:1111.0730 \[gr-qc\]](#).
- [71] P. S. Letelier and S. R. Oliveira, “On uniformly accelerated black holes,” *Phys. Rev. D* **64** (2001) 064005, [arXiv:gr-qc/9809089](#).

- [72] J. Bicak and V. Pravda, “Spinning C metric: Radiative space-time with accelerating, rotating black holes,” *Phys. Rev. D* **60** (1999) 044004, [arXiv:gr-qc/9902075](#).
- [73] J. Podolsky and J. B. Griffiths, “Null limits of the C metric,” *Gen. Rel. Grav.* **33** (2001) 59–64, [arXiv:gr-qc/0006093](#).
- [74] V. Pravda and A. Pravdova, “Coaccelerated particles in the C metric,” *Class. Quant. Grav.* **18** (2001) 1205–1216, [arXiv:gr-qc/0010051](#).
- [75] O. J. C. Dias and J. P. S. Lemos, “Pair of accelerated black holes in anti-de Sitter background: AdS C metric,” *Phys. Rev. D* **67** (2003) 064001, [arXiv:hep-th/0210065](#).
- [76] J. B. Griffiths and J. Podolsky, “A New look at the Plebanski-Demianski family of solutions,” *Int. J. Mod. Phys. D* **15** (2006) 335–370, [arXiv:gr-qc/0511091](#).
- [77] P. Krtous, “Accelerated black holes in an anti-de Sitter universe,” *Phys. Rev. D* **72** (2005) 124019, [arXiv:gr-qc/0510101](#).
- [78] F. Dowker, J. P. Gauntlett, D. A. Kastor, and J. H. Traschen, “Pair creation of dilaton black holes,” *Phys. Rev. D* **49** (1994) 2909–2917, [arXiv:hep-th/9309075](#).
- [79] R. Emparan, G. T. Horowitz, and R. C. Myers, “Exact description of black holes on branes. 2. Comparison with BTZ black holes and black strings,” *JHEP* **01** (2000) 021, [arXiv:hep-th/9912135](#).
- [80] R. Emparan, G. T. Horowitz, and R. C. Myers, “Exact description of black holes on branes,” *JHEP* **01** (2000) 007, [arXiv:hep-th/9911043](#).
- [81] R. Emparan, R. Gregory, and C. Santos, “Black holes on thick branes,” *Phys. Rev. D* **63** (2001) 104022, [arXiv:hep-th/0012100](#).
- [82] R. Gregory, S. F. Ross, and R. Zegers, “Classical and quantum gravity of brane black holes,” *JHEP* **09** (2008) 029, [arXiv:0802.2037 \[hep-th\]](#).
- [83] G. Arenas-Henriquez, R. Gregory, and A. Scoins, “On acceleration in three dimensions,” *JHEP* **05** (2022) 063, [arXiv:2202.08823 \[hep-th\]](#).
- [84] G. Arenas-Henriquez, A. Cisterna, F. Diaz, and R. Gregory, “Accelerating Black Holes in 2 + 1 dimensions: Holography revisited,” *JHEP* **09** (2023) 122, [arXiv:2308.00613 \[hep-th\]](#).
- [85] G. Arenas-Henriquez, *Many Phases of Accelerating Black Holes in 2+1 Dimensions*. PhD thesis, Durham U., Durham U., 2023.
- [86] J. Tian and T. Lai, “Thermodynamics and Holography of Three-dimensional Accelerating black holes,” [arXiv:2312.13718 \[hep-th\]](#).

- [87] J. Tian and T. Lai, “Aspects of three-dimensional C-metric,” *JHEP* **03** (2024) 079, [arXiv:2401.04457 \[hep-th\]](#).
- [88] S. He and H. Shu, “Correlation functions, entanglement and chaos in the $T\bar{T}/J\bar{T}$ -deformed CFTs,” *JHEP* **02** (2020) 088, [arXiv:1907.12603 \[hep-th\]](#).
- [89] B. Chen, L. Chen, and P.-X. Hao, “Entanglement entropy in $T\bar{T}$ -deformed CFT,” *Phys. Rev. D* **98** no. 8, (2018) 086025, [arXiv:1807.08293 \[hep-th\]](#).